

Your Ref :

Our Ref:CD/FSSD/12/02/03/01

Date : 16 Sep 2016

Registrar, Board of Architects
Registrar, Professional Engineers Board
President, Singapore Institute of Architects
President, Institution of Engineers, Singapore
President, Association of Consulting Engineers, Singapore

Dear Sir/Mdm

SCI PUBLICATIONS P288 AND P390 FOR FIRE SAFETY DESIGN OF MULTI-STOREY STEEL-FRAMED BUILDINGS WITH COMPOSITE SLABS

Currently, the Fire Code requires any element of structure to have fire resistance in compliance with Clauses 3.3 and 3.4. Fire protection is thus required for structural steel elements, including secondary steel beams.

2. The SCI Publication P288 titled "Fire Safety Design: A new approach to multi-storey steel-framed buildings" allows a Performance-Based (PB) approach to fire safety design of multi-storey steel-framed buildings with composite slabs. The publication provides information on building structural behaviour and identifies steel members which do not require fire protection. It is used in conjunction with SCI Publication 390 titled "TSLAB v3.0 User Guidance and Engineering Update" and its accompanying software TSLAB v3.0. Many buildings in UK have since benefited from the application of SCI Publications P288 and P390, resulting in reduced fire protection cost and improved construction productivity (e.g. no fire protection required for secondary steel beams).

3. SCDF does not have objection to the adoption of such design approach by building practitioners provided the building is sprinkler-protected and the unprotected beams shall be designed and detailed with embedded shear studs. Building



SCDF – A member of the Home Team

practitioners are also advised to use the SCI Publications P288 and P390 together with the Design Commentary published by Nanyang Technological University (Annex A). Such plans of fire safety works shall be submitted to SCDF under the PB regulatory system.

4. Please convey the contents of this circular to members of your Board / Institution /Association. This circular is also available in CORENET-e-Info: <http://www.corenet.gov.sg/einfo>. For any clarification, please contact: LTC Chong Kim Yuan at DID: 68481476 or email: Chong_Kim_Yuan @ scdf.gov.sg.

Yours faithfully,

(transmitted via e-mail)
MAJ Tan Chung Yee
Fire Safety & Shelter Department
for Commissioner
Singapore Civil Defence Force

Distribution list

CEO, BCA
CEO, URA
CEO, HDB
CEO, JTC
CE, LTA
CE, SPRING Singapore
President, REDAS
President, IFE
President, SISV
President, FSMAS
President, SCAL
Honorary Secretary, SPM
SCDF Fire Safety Standing Committee
Fire Code Review Committee



SCDF – A member of the Home Team

Annex A

DESIGN COMMENTARY ON SCI PUBLICATIONS P288 AND P390

DESIGN COMMENTARY ON SCI PUBLICATIONS P288 AND P390



Prof TAN Kang Hai - Dr NGUYEN Tuan Trung - Mr LIU Junxian

School of Civil and Environmental Engineering
Nanyang Technological University

DESIGN COMMENTARY ON SCI PUBLICATIONS P288 AND P390

**Prof TAN Kang Hai
Dr NGUYEN Tuan Trung
Mr LIU Junxian**

School of Civil and Environmental Engineering
Nanyang Technological University

2014

TABLE OF CONTENTS

1	Introduction	1
1.1	Background	1
1.2	SCI Publications P288 and P390	1
1.3	Objectives and Scope of work	2
2	Basis of design.....	4
2.1	Safety	4
2.2	Type of structures	4
3	Recommendations for structural elements	9
3.1	Floor slab and beams	9
3.2	Design of edge beams.....	12
3.3	Beams above fire resistant walls	13
3.4	Columns.....	14
3.5	Connections	14
3.6	Overall building stability	15
4	Calibration of P288 and P390 against the fire tests conducted in Nanyang Technological University	16
4.1	Introduction.....	16
4.2	Discussions on the Bailey-BRE method	16
4.3	Calibration of the Bailey-BRE method against NTU fire tests.....	20
4.3.1	Test programme in NTU.....	20
4.3.2	Comparison principles	25
4.3.3	Summary of comparison results	28
4.4	Conclusions.....	31
5	Conclusions	32
	Appendix A The Bailey-BRE method	
	Appendix B Estimation of cost saving of fire protection for a typical composite floor	
	Appendix C Calibration of P288 against NTU fire tests	

SCI Publications P288 and P390 Commentary – Reading key

Corresponding parts commented

PART A P288

2.2 Type of structures



Section 2.2 of P288

SECTION 2 BASIS OF DESIGN

2.2 (C) Type of structures



Comment on Part A Section 2.2

2.2.1 (CL) Simple joint models



Clarification for Section 2.2.1

Corresponding part commented

PART A P288

3.1.4 Effect of additional load on boundary beams [P390 Pt2 1]



Part A Section 3.1.4 of P288



Complemented information for P288 given in P390 Part 2 Section 1

SECTION 3 RECOMMENDATIONS FOR STRUCTURAL ELEMENTS

3.1.4 (C) Effect of additional load on boundary beams [C-P390 Pt2 1]



Comment on Part A Section 3.1.4 of P288



Comment on complemented information in P390 Part 2 Section 1

1 INTRODUCTION

1.1 Background

Over the past two decades, multi-storey steel-framed buildings with composite steel deck – concrete slab systems in Singapore have been designed in accordance with BS 5950 both at normal and elevated temperatures. This standard has now been replaced by EN 1994-1-1 [1], EN 1994-1-2 [2] and Singapore Standards (SS EN 1994-1-1:2004 and SS EN 1994-1-2:2005) since April 2013. This transition requires further research studies focusing on the advanced methods mentioned in the Eurocodes.

The fire design methodology in Eurocodes allows engineers to have greater flexibility in their approach. Two permitted approaches in EN 1994-1-2 include *prescriptive* and *performance-based approaches*. The prescriptive approach is based on nominal fires while the performance-based approach refers to thermal actions generated based on actual compartment fire characteristics.

One of the advantages of performance-based approach is to allow engineers to select simple or advanced fire models to design structures under more realistic fire conditions, provided that these fire models have been validated by experimental tests. As a result, structural fire protection cost can be reduced.

This commentary is concerned with the design of multi-storey steel-framed buildings with composite steel deck – concrete slab systems under fire conditions using the advanced method based on the concept of tensile membrane action (TMA) developed in the concrete slab at large deflections, aiming to reduce fire protection cost for the steel-framed composite buildings without compromising on structural safety.

1.2 SCI Publications P288 and P390

SCI Publication P288 “Fire Safety Design: A new approach to multi-storey buildings” [3] (referred in this document as P288) sets out the design philosophy for the Bailey-BRE method, while SCI Publication P390 “TSLAB v3.0 User Guidance and Engineering Update” [4] (referred as P390) provides the information on the operation of

the TSLAB software v3.0. This software tool has been developed by SCI to facilitate the Bailey-BRE method. Both P288 and P390 must be used together when applying the simple method to design steel-framed buildings with composite slabs. Engineers may consider using TSLAB v3.0 software to facilitate design. Many buildings in the UK have since benefited from the application of the simple design method, resulting in reduced fire protection costs [3]. P288 has been developed based on extensive results from fire tests, ambient temperature tests and finite element analyses.

SCI P390 has incorporated Eurocode requirements. It includes verification for the edge beam capacity and modified mesh temperature. With the latest release of P390, a number of Sections in P288 are updated or no longer applicable as shown in **Table 1**.

Table 1 Contents updated in P390 compared to P288

<i>P288</i>	<i>Corresponding part in P390</i>	<i>Contents updated</i>
Section 3 Part A	Section 1 Part 2	<ul style="list-style-type: none"> - Provide recommendations for structural design of the floor plate - Complement the information given in Section 3 Part A of P288. - Replace Section 3.1.5 of P288 which covers the effect of additional load on boundary beams.
Section 3.2 Part A	Section 2 Part 2	<ul style="list-style-type: none"> - Provide information on design of fire-protected beams on the perimeter of each floor design zone. - Complement the basic information given in Section 3.2 Part A of P288

1.3 Objectives and Scope of work

The SCI Publications P288 and P390 and this commentary shall not be used to replace SS EN 1994-1-1:2004 and SS EN 1994-1-2:2005 in the design of composite steel-frame buildings under fire conditions. They only provide design guidance on an advanced

calculation method that engineers may use in the design of composite steel-framed buildings. In addition, all the detailing clauses in SS EN 1994-1-1:2004 at ambient design such as anchoring for steel mesh, shear stud design, stud spacing, etc. shall be complied.

Although widely applied in the UK, enhancement of fire resistance provided by the TMA is still a very new concept for structural engineers and regulatory authority in Singapore. To disseminate the design concept using TMA to these potential users, this document aims to provide commentary and clarifications for the SCI Publications P288 and P390 including:

- Commentary on each section of SCI Publications P288 and P390 (**Sections 2 and 3**);
- Discussions on the Bailey-BRE method which forms the basis for P288 and P390 (**Section 4**);
- Validation of the Bailey-BRE method using the small scale fire tests conducted in Nanyang Technological University (**Section 4**).

2.1 Safety

No comment is added.

2.2 Type of structures

2.2 (C) Type of structures

The guidance **does not** apply to:

- (1) Floors constructed using precast concrete slabs;
- (2) Internal floor beams that have been designed to act non-compositely (beams at the edge of the floor slab may be non-composite);
- (3) Beams with service openings, *i.e.* composite floor with cellular beams;
- (4) Flat slab systems.
- (5) Warehouses and car parks. This guidance only applies to offices and residential buildings with imposed loads less than or equal to 4 kPa.
- (6) Composite slabs that require above 2-h fire resistance

For the above-mentioned types of buildings, the guidance shall not be applied until further research has been conducted in Singapore showing the applicability of the method.

2.2.1 (CL) Simple joint models

The joint models given in P288 assume that bending moments are not transferred through the joints. The joints are known as ‘simple joints’.

Beam-to-column joints that may be considered as ‘simple’ include joints with the following components:

- flexible end plates (**Fig. 1**)
- fin plates (**Fig. 2**)
- web cleats (**Fig. 3**)

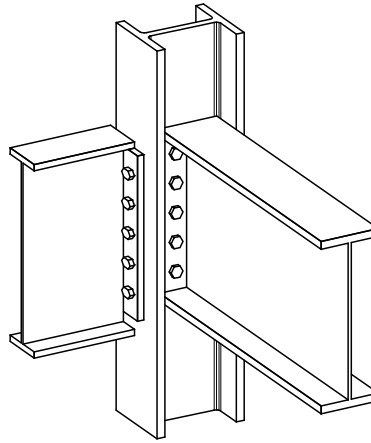


Fig. 1 Joint with flexible end plate connections

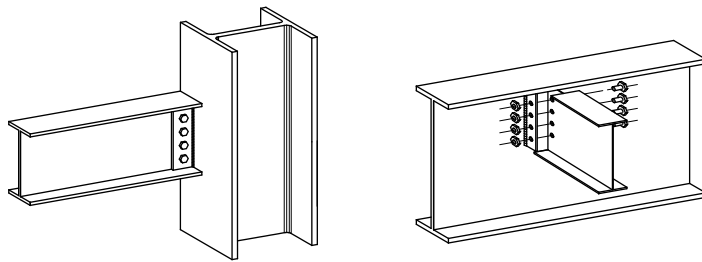


Fig. 2 Joints with fin plate connections

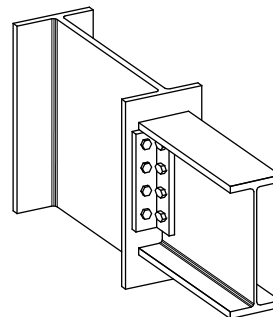


Fig. 3 Joint with a web cleat connection

2.2.2 (CL) Floor slabs and beams

The design recommendations given in P288 are applicable to composite floor slabs which consist of steel sheeting, reinforcing mesh and normal or lightweight concrete. Resistance of the steel decking is ignored in the design method under fire conditions, but the presence of the steel decking prevents concrete spalling on the underside of the slab.

The design method can be used with either isotropic or orthotropic reinforcing mesh, that is, meshes with either the same or different reinforcement ratios in orthogonal directions. Steel grade for the mesh reinforcement should be specified in accordance with EN 10080. The design method can only be used for welded mesh reinforcement and cannot consider more than one layer of reinforcement. Reinforcement bars in the ribs of the composite slab are **not** considered in the calculations.

The beam sizes, *i.e.* primary and secondary beams, shall be designed according to the requirements of SS EN 1994-1-1 at ambient temperatures, and are checked in accordance with the design method at elevated temperatures. The checking process is given in Section 2 of SCI P390.

2.2.3 (CL) Fire exposure

The recommendations given in the Bailey-BRE method may be applied to buildings in which structural elements are exposed to the standard temperature-time curve or parametric temperature-time curve, both as defined in EN 1991-1-2 [5].

Advanced models, *e.g.* finite element models, may also be used to define a temperature-time curve for a natural fire scenario. The resulting temperature-time curve may be used as the input data for the design method.

SCI recommends that only engineers familiar with fire safety engineering should attempt to use any information based on parametric fire curves. This is also the recommendation from Singapore design commentary.

In all cases, the normal provisions of national regulations regarding the means of escape should be followed.

2.2.4 (CL) Combination of actions

The combinations of actions for accidental design situations given in Clause 6.4.3.3 and Table A1.3 of EN1990 [6] should be used for fire limit state verifications. With only unfavourable permanent actions and no prestressing actions present, the combination of actions to consider is:

$$\sum G_{k,j,\text{sup}} + A_d + (\psi_{1,1} \text{ or } \psi_{2,1}) Q_{k,1} + \sum \psi_{2,i} Q_{k,i}$$

where:

$G_{k,j,\text{sup}}$: unfavourable permanent action (j^{th} value)

A_d : accidental action;

$Q_{k,1}$ and $Q_{k,i}$: accompanying variable actions, leading and the others, respectively;

$\psi_{1,1}$: factor for the frequent value of the leading variable action;

$\psi_{2,i}$: factor for the quasi-permanent value of the i^{th} variable action.

The use of factor $\psi_{1,1}$ or $\psi_{2,i}$ depends on which set of combinations is used. Factor $\psi_{1,1}$ is used for the frequent value of leading variable action, whereas factor $\psi_{2,i}$ is used for the quasi-permanent value of i^{th} variable action. All the values for ψ factors should be in accordance with the Singapore National (SS) Annex to EN1990 as shown in **Table 2**.

The Eurocode recommended the values for imposed loads on floors in EN 1991-1-1 given in SS EN 1991-1-1.

Table 2 Values of ψ factors recommended in SS EN 1990

Actions	SS EN 1990	
	ψ_1	ψ_2
Domestic, office and traffic areas where:		
30 kN < vehicle weight ≤ 160 kN	0.5	0.3
Other*		0.6
	0.7	

* climatic actions are not included

3.1 Floor slab and beams

3.1.1 Reinforcing mesh

No comment is added.

3.1.2 Floor design zones

3.1.2 (C) Floor design zones

The criteria to divide each floor into a number of floor design zones mentioned in Section 3.1.2 P288 shall be followed closely.

The previous tests [7, 8] as well as the tests conducted in Nanyang Technological University [9] show that these criteria are conservative and realistic.

3.1.3 Information in Design Tables

3.1.3 (C) Information in Design Tables

The required criteria for using the Design Tables mentioned in Section 3.1.4 of P288 shall be followed. These tables provide initial estimates of required reinforcement area for a predetermined fire resistance period.

Restrictions of the use of the Design Tables are as follows:

- The tables are for fire resistance of 30, 60, 90 and 120 minutes. No information is given for 180 and 240 minutes.
- Only limited values of applied loads are mentioned.
- The tables are applicable to profiled steel decking up to 70 mm deep and for depths of concrete above the steel decking from 60 to 80 mm.

- The tables for standard A and B series meshes may be used to check only the slab resistance. **For the design of the edge beams, please refer to Section 3.2.**

For cases outside the scope of the Design Tables, a full fire engineering analysis of the floor using the model developed by Prof. Bailey (Appendix B of P390) may be used directly. Alternatively, advanced calculation models may be used.

3.1.4 Reinforcement [P390 Pt2 1.5]

3.1.4 (C) Reinforcement

The yield strength and ductility of the reinforcing steel material should be specified in accordance with the requirements of SS EN 10080. The characteristic yield strength of reinforcement to SS EN 10080 will be at 500Pa.

In order that the reinforcement has sufficient ductility to allow the development of TMA, Class B or Class C reinforcement should be specified. Class A reinforcement should not be used.

Available reinforcing steel materials in the national market can be used provided that they conform to the requirements of SS EN 10080, particularly with regard to the yield strength and ductility.

3.1.5 Effect of additional load on boundary beams

3.1.5 (C) Effect of additional load on boundary beams

This section is replaced by Section 1.4.2 Part 2 of P390. More details are given in Section 3.2.

3.1.6 Temperature calculation of unprotected composite slabs

3.1.6 (CL) Temperature calculation of unprotected composite slabs

The temperature distribution in a composite slab can be determined using a calculation model by finite difference method or finite element approach taking into account the exact shape of the slab and respecting the rules 4.4.2 of EN 1994-1-2.

As an alternative, the temperature distribution in unprotected composite slabs subject to the standard fire can be determined from semi-analytical models.

A semi-analytical model is adopted in TLAB V3.0 which uses a 2D finite difference heat transfer method (Appendix A of SCI P390). This method has been used for many years by SCI to predict the temperature distributions in steel and steel-concrete composite cross sections and has been shown to give reasonably accurate predictions of the behaviour of sections in fire resistance tests.

Another semi-analytical model is the method stipulated in EN 1994-1-2 Annex D. However, the Building and Construction Standards Committee responsible for SS EN 1994-1-2 [10] does not recommend the use of Annex D. This is because modelling has shown that the method given in EN 1994-1-2 Annex D is too conservative for profiled sheeting shapes containing large stiffeners or indentations. The SS NA advised that guidance is available on www.steel-ncci.co.uk that offers an alternative to Annex D where temperatures of the strips required for plastic analysis of the section are given

directly by a series of cross-sectional-depth-temperature relationships in equation form. A cross-sectional-depth-temperature relationship is also provided to calculate the temperature of reinforcing bars within the ribs of the slab.

Therefore, the Eurocodes Non Contradictory Complementary Information (NCCI) for fire resistance design of composite slabs [11] can be used to determine the temperature distribution in unprotected composite slabs subjected to standard fire. Thereafter, the load-bearing capacity of the slabs is calculated based on the Bailey-BRE method.

3.1.7 Temperature calculation of unprotected composite beams

3.1.7 (CL) Temperature calculation of unprotected composite beams

The method given in SS EN 1994-1-2, Section 4.3.4.2.2, can be used to determine temperature of unprotected steel beams.

3.2 Design of edge beams

3.2 (C) Design of edge beams

The design method to determine the load bearing capacity of the floor design zone is described in Appendix B of P390. The perimeter beams which bound each floor design zone must be designed to achieve the period of fire resistance required by the floor slab. This will ensure that the pattern of yield lines and the associated enhancement due to tensile membrane action can actually happen in practice.

The required moment of resistance of the edge beams is calculated by considering alternative yield line patterns

that would allow the slab to fold along an axis of symmetry without developing tensile membrane action. Details of the calculation method are given in Section 2 of SCI Publication P390. This procedure shall be followed.

On the other hand, when tensile membrane action is mobilised, the secondary and main edge protected beams carry more load at the fire limit state as shown in **Fig. 4**. Therefore, the load ratio of the protected edge beams increases. *This must be considered in calculating the required moment capacity of these beams to ensure that they provide sufficient support to allow the development of tensile membrane action in the slabs.* A critical temperature for the beams can then be calculated and appropriate levels of fire protection can be applied to ensure that this critical temperature is not exceeded during the required fire resistance.

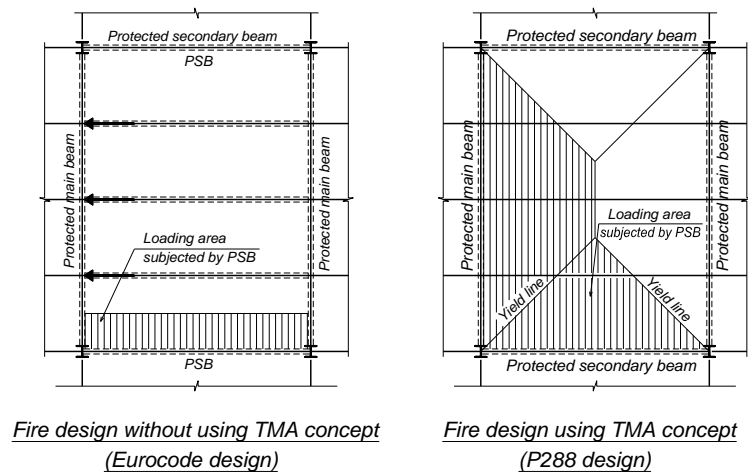


Fig. 4 Load carried by edge beams at fire limit stage

3.3 Beams above fire resistant walls

No comment is added.

3.4 Columns

No comment is added.

3.5 Connections

3.5 (C) Connections

Types of connections

As stated in Section CL2.2.1 ‘simple’ joints such as those with flexible end plates, fin plates and web cleats shall be used when adopting the simple design method.

The steel frame building tested at Cardington contained flexible end plate and fin plate connections. Partial and full failures of some of the joints were observed during the cooling phase of the Cardington fire tests; however, these failures did not result in collapse of the structure.

In the case where the plate was torn off from the end of the beam, no collapse occurred because the floor slab transferred the shear to other load paths. This highlights the important role of the composite floor slab, which can be achieved with proper lapping of reinforcement in the slab.

The resistance of simple joint should be verified using the rules given in EN 1993-1-8 [12]. To ensure that a joint does not transfer significant bending moment and that it is indeed a ‘simple’ joint, it must have sufficient rotation capacity. This can be achieved by detailing the joint such that it meets geometrical limits. Guidance on geometrical limits and initial sizing to ensure sufficient rotation capacity of the joint is given in Access-steel documents SN013 and SN016 [13, 14].

Fire protection of connections

In cases where both structural members to be connected are fire protected, the protection appropriate to each member should be applied to the parts of the plates or angles in contact with that member. If only one member requires fire protection, the plates or angles in contact with the unprotected member may be left unprotected.

3.6 Overall building stability

No comment is added.

4 CALIBRATION OF P288 AND P390 AGAINST THE FIRE TESTS CONDUCTED IN NANYANG TECHNOLOGICAL UNIVERSITY

4.1 Introduction

This section aims to provide discussions on the fundamental assumptions of the Bailey-BRE method (also referred as ‘the simple design method’ in SCI Publication P288). To ascertain the use of simple design method and to enlarge its application in Singapore, a project funded by A*Star Singapore has been conducted in Nanyang Technological University (NTU) in order to:

- Verify the assumptions of the simple design method that the protected edge beams are vertically supported at all times during the fire.
- Verify the use of the simple design method in performance-based fire engineering design of composite slab-beam floor systems.

Comparisons between the test results and those predicted by the Bailey-BRE method are summarised in **Sections 4.3** and **4.4**. Details of the comparisons can be found in **Appendix C**. Conclusions are given in **Section 4.5**.

4.2 Discussions on the Bailey-BRE method

The Bailey-BRE method [15] presented in SCI Publication P288 begins by dividing a composite floor into several horizontally-unrestrained, vertically supported slab panels – *floor design zones* (**Fig. 5**). Each of these floor design zones consists of simply-supported unprotected interior beams. As temperature increases, the formation of plastic hinges in the interior beams re-distributes the loads to the two-way bending slab which undergoes large vertical deflections. Based on rigid-plastic theory with large change of geometry, the additional slab capacity provided by tensile membrane action is calculated as an enhancement to the conventional yield-line capacity.

The Bailey-BRE method was developed mainly on the basis of full scale natural fire tests in which the floors were subjected to fully developed compartment fires. The first question here is whether the simple design method could be applied to fire design using the standard temperature-time curve (ISO 834 fire curve).

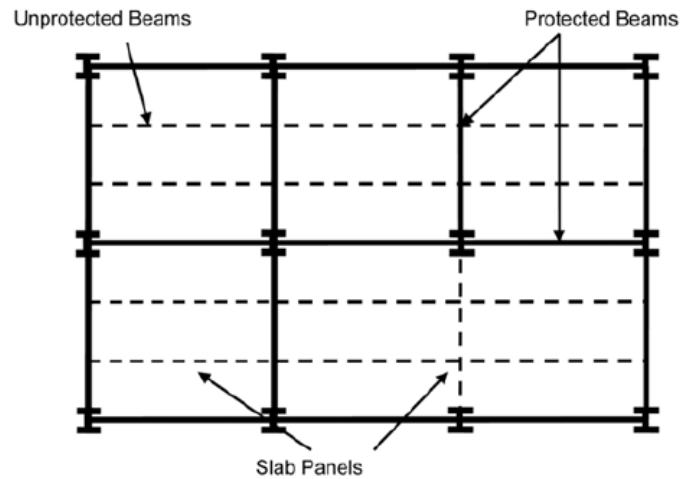


Fig. 5 Typical slab panels

This question has been answered by a research project named “Fire resistance assessment of partially protected composite floors (FRACOF)” conducted in France in 2008 [16]. The FRACOF fire test was intended to provide experimental evidence on the behaviour of composite slab-beam floor systems exposed to the ISO 834 fire curve and to widen the application of the simple design method in France. The test results showed that the whole floor remained structurally robust under a duration of 120 minutes as expected, despite the fracture of steel mesh reinforcement in the concrete slab. After that, a design guide named “FRACOF design guide” was released. Therefore, it can be concluded that the simple design method can be applied to fire design using the ISO 834 fire curve.

The design procedure is presented in **Fig. 6**.

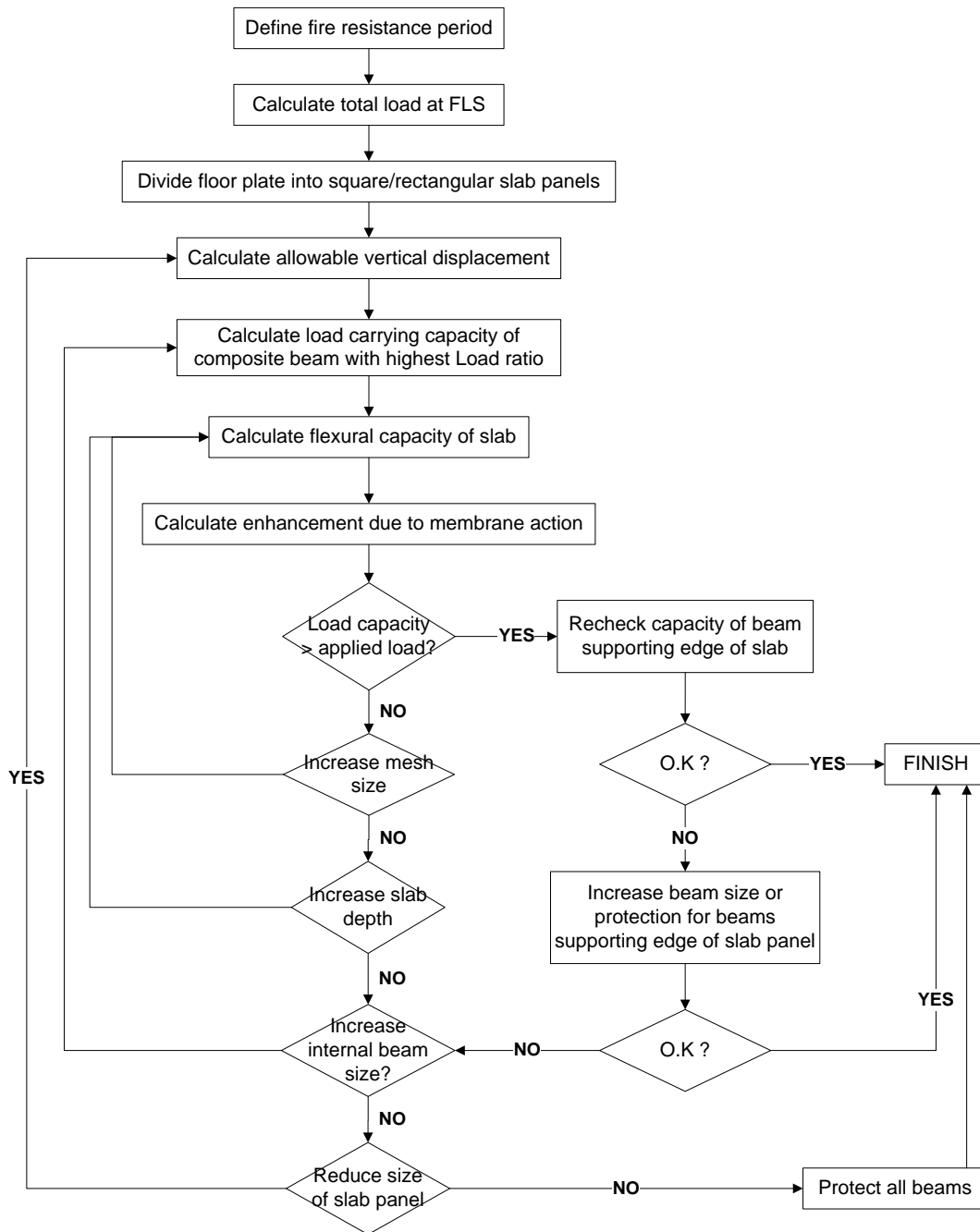


Fig. 6 Design procedure of the Bailey-BRE method [17]

By assuming that under tensile membrane action stage, the dominant load-carrying capacity of the system is due to the composite slab, the following assumptions have been used in the Bailey-BRE method:

1. The load carried by the flexural behaviour of the grillage of composite beams within the fire compartment, is based on plastic mechanism for the beam with

the highest Load Ratio (i.e. the beam which will 'fail' first in the fire). The beams are assumed to be simply-supported.

2. The load supported by the flexural behaviour of the composite slab is calculated based on the yield-line mechanism of the slab, assuming that the edge and interior beams have zero resistance.
3. The enhancement due to membrane action in the composite slab (e factor) is based on the yield-line mechanism of the slab.
4. The load-carrying capacity of the composite beams and slab (enhanced due to membrane action) are added together.
5. *Important implicit assumption:* the protected edge beams are vertically supported at all times during the fire. The task of providing the necessary vertical support requires protecting the edge beams of a slab panel to achieve a required temperature at a required fire resistance. They should also have sufficient rigidity during the fire limit state.

These aforementioned assumptions seem to be conservative at the first glance. However, the 4th and 5th assumptions require further examinations. As reported in Tan *et al.* [9], deflections of the protected edge beams at failure of the slab were significant, about 40mm (1/56 span) with a beam span of 2.25m.

Based on the 4th assumption, the capacity of the *unprotected composite interior beams* is added to the enhanced slab capacity, provided that these beams have not failed yet. Therefore, it is required to check the bending moment capacity of unprotected interior beams under fire conditions.

In the simple design method, a deflection limit has to be assumed, and then the enhancement above the yield-line load bearing capacity of the slab due to tensile membrane action is calculated based on that deflection. Details of calculation of the Bailey-BRE method can be found in Appendix B of SCI P390 [4]. The deflection limit proposed by Bailey *et al.* [15] is estimated by combining the components due to thermal curvature and strain in the reinforcement using Eq. (1). This deflection limit was proposed based on a pragmatic approach where a limit is defined for the average strain

in the reinforcement. Therefore, this deflection limit is explicitly independent of load ratio.

$$w = \frac{\alpha(T_2 - T_1)l^2}{19.2h} + \sqrt{\left(\frac{0.5f_y}{E_s}\right)_{\text{Reinf}_{20^\circ\text{C}}}} \frac{3L^2}{8} < w_{\text{max}} = \frac{\alpha(T_2 - T_1)l^2}{19.2h} + \frac{l}{30} \quad (1)$$

where α is the coefficient of thermal expansion (12×10^{-6} for normal weight concrete; T_2 and T_1 are the bottom and top surface temperatures of the slab respectively; h is the average depth of the concrete slab; l and L are the shorter and longer spans of the slab panel; f_y and E_s are the yield and elastic modulus of the reinforcing steel at ambient temperature.

Based on the Cardington fire test, Bailey proposed that $(T_2 - T_1)$ was equal to 770°C for fire exposure below 90 minutes and 900°C thereafter. This value was obtained from the test data from the Cardington fire tests [18] and referred hereafter as *the P288 deflection limit*. In P390 [4], an update of P288, the deflection limit is also calculated by Eq. (1), except that the term $(T_2 - T_1)$ is based on the temperatures calculated at the bottom and top surfaces of the slab at each time step (referred hereafter as *the P390 deflection limit*). The difference between the two deflection limits highlights the effect of recent changes to the Bailey-BRE method [19].

Therefore, *the first step* of the present investigation is to check whether the deflection limits, *i.e.* the P288 and P390 deflection limits, are satisfied against the test results conducted in NTU. *The second step* is to compare the slab load-bearing capacity predicted by the Bailey-BRE method against the test results. Details of the comparisons can be found in **Sections 4.3** and **4.4**.

4.3 Calibration of the Bailey-BRE method against NTU fire tests

4.3.1 Test programme in NTU

The test programme conducted in NTU from 2010 to 2012 included five series with 17 composite beam-slab floor systems in total, which were tested under fire conditions to study the development of tensile membrane action (TMA) in the composite beam-slab

systems. Only brief information of the tested specimens is provided here. Details of the test results and discussions can be found in **Appendix C** and the project report [9].

The specimens were of *one-quarter scale* due to limitations of laboratory facility and space. For interior slab panels, the slabs extended 0.45m around all four edges. Shrinkage reinforcement mesh with a grid size of 80mm x 80mm and a diameter of 3mm (giving a reinforcement ratio of 0.16%) was placed at about 38mm below the slab top surface, which was ensured by 40mm x 40mm concrete supporting blocks, placed at a spacing of 320mm x 320mm. The 0.16% reinforcement ratio is close to the minimum value required by EN 1994-1-1 (0.2% for un-propped construction). The mesh was continuous across the whole slab, with no lapping of mesh. The specimens were cast using ready-mixed concrete, with the aggregate size ranging from 5 to 10mm, to enable adequate compaction during placement.

All specimens were designed at elevated temperatures by using the fire protection strategy for members recommended in the SCI Publication P288. Therefore, all the edge beams and the columns were protected to a prescriptive one-hour fire-protection rating. No fire-proofing material was applied to the interior beams and the underside of the decking.

Due to 1:4 scaling there was no standard steel decking suitable for the slabs. To protect the heating elements from concrete spalling, the slabs were cast onto a 2mm thick steel sheet. The contribution of this sheet to the slab's load-bearing capacity was ignored, since the unprotected sheet would de-bond from the concrete slab, as observed in previous studies.

Series I and II

The first two series (Series I and II) included eight *interior slab panels*. The aim was to study the effects of unprotected interior secondary beams and of rotational restraint on the development of TMA. Test series I and II can be divided into two groups. *Group 1* consisted of two specimens, namely, S1 and S3-FR, which had no interior beams (**Fig.**

7). Group 2 consisted of six specimens which had two interior beams (**Fig. 8**). Table 3 presents the details of Series I and II specimens.

Table 3 Specimen details – Series I and II

Series	$L \times W \times h$ (mm)	Aspect ratio	Main beam	Protected secondary beam	Unprotected secondary beam	
I	S1	2250x2250x55	1.0	W130x130x28.1	Built-up 80x80x17.3	n.a.
	S2-FR-IB	2250x2250x55	1.0	W130x130x28.1	Built-up 80x80x17.3	Built-up 80x80x17.3
	S3-FR	2250x2250x58	1.0	W130x130x28.1	Built-up 80x80x17.3	n.a.
II	P215- M1099	2250x2250x57	1.0	W130x130x28.1	Built-up 80x80x17.3	Built-up 80x80x17.3
	P368- M1099	2250x2250x58	1.0	W130x130x28.1	Built-up 100x80x18.8	Built-up 80x80x17.3
	P486- M1099	2250x2250x55	1.0	W130x130x28.1	Joists 102x102x23	Built-up 80x80x17.3
	P215- M1356	2250x2250x58	1.0	UB 178x102x19	Built-up 80x80x17.3	Built-up 80x80x17.3
	P215- M2110	2250x2250x59	1.0	UB 203x102x23	Built-up 100x80x18.8	Built-up 80x80x17.3

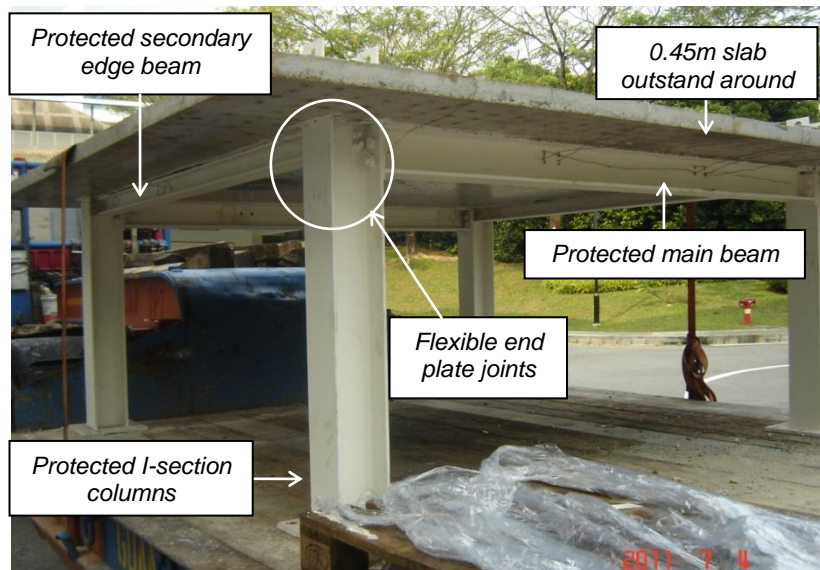


Fig. 7 Typical specimen without interior beams

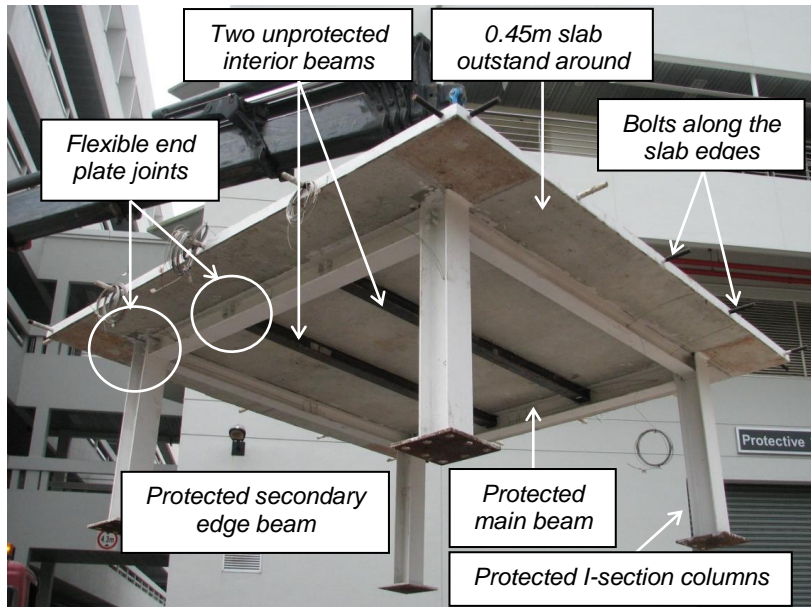


Fig. 8 Typical specimen with two unprotected interior beams

Series III, IV and V

Series III, IV and V included 9 specimens in total. The parameters investigated were the slab aspect ratio and boundary continuity. Series III focused on isolated composite slab-beam systems with no boundary continuity while Series IV & V studied various boundary conditions, such as interior (four continuous edges), edge (three continuous edges) and corner (only two continuous edges) panels (**Fig. 9**). For Series IV and V, aspect ratios of 1.0 and 1.5 were also considered respectively, as shown in **Table 4**.

Table 4 Specimen details – Series III, IV and V

<i>Series</i>	<i>Specimen</i>	<i>L x W x h (mm)</i>	<i>Aspect ratio</i>	<i>Supporting steel beams</i>
III	ISOCS1	2250x2250x60	1.0	Joist 102x102x23 kg/m
	ISOCS2	2250x2250x60	1.0	Joist 102x102x23 kg/m
	ISOCS3	2250x1500x60	1.5	Joist 102x102x23 kg/m
IV	ICS1	2250x2250x60	1.0	Joist 102x102x23 kg/m
	ECS1	2250x2250x60	1.0	Joist 102x102x23 kg/m
	CCS1	2250x2250x60	1.0	Joist 102x102x23 kg/m
V	ICS2	2250x1500x60	1.5	Joist 102x102x23 kg/m
	ECS2	2250x1500x60	1.5	Joist 102x102x23 kg/m
	CCS2	2250x1500x60	1.5	Joist 102x102x23 kg/m

where L, W and h are the length, width and thickness of the slab, respectively; ISOCS, ICS, ECS and CCS refer to isolated, interior, edge and corner composite slabs, respectively.

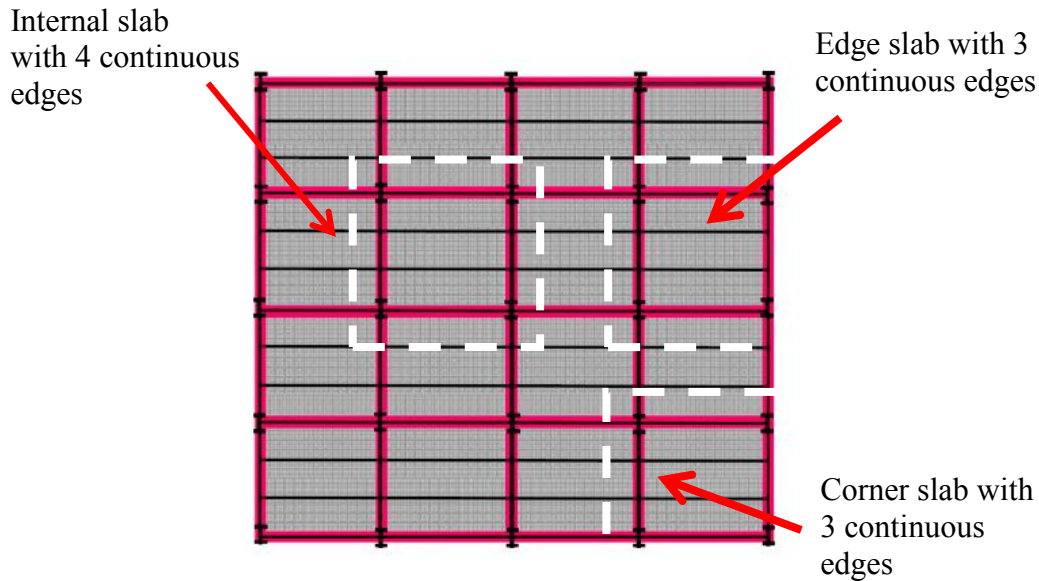


Fig. 9 Typical building layout with different boundary conditions

In order to simulate the boundary continuity, embedded M25 bolts (**Fig. 8**) were tied to surrounding restrained frames to ensure the boundary lines remained straight without any movement for both compressive membrane action and tensile membrane action. Moreover, the contacting area between these M25 bolts and concrete was larger than that between the $\Phi 6$ mm mesh and concrete, which was to ensure the edge continuity.

Typical test setup and test load

Fig. 10 shows a typical test setup. Due to large dimensions of the furnace (3m long x 3m wide x 0.75m high), it could not simulate the ISO 834 standard fire curve. Its heating rate is about $20^{\circ}\text{C}/\text{min}$, which is within the practical range of heating rate for steel sections as stipulated in BS 5950-8 [20]. As discussed in **Section 4.2**, the simple design method can be applied for both compartment and standard (ISO 834) fire curves.

All specimens were loaded up to a predetermined value ($15.8\text{kN}/\text{m}^2$ for series I and II, $20\text{kN}/\text{m}^2$ for Series III and IV, and $30\text{kN}/\text{m}^2$ for Series V). These values corresponded

to 0.4 to 0.6 of the yield-line load at ambient temperature for specimens with interior beams, and 1.9 for specimens without interior beams. After that, the load was kept constant and temperature was increased until failure was identified.

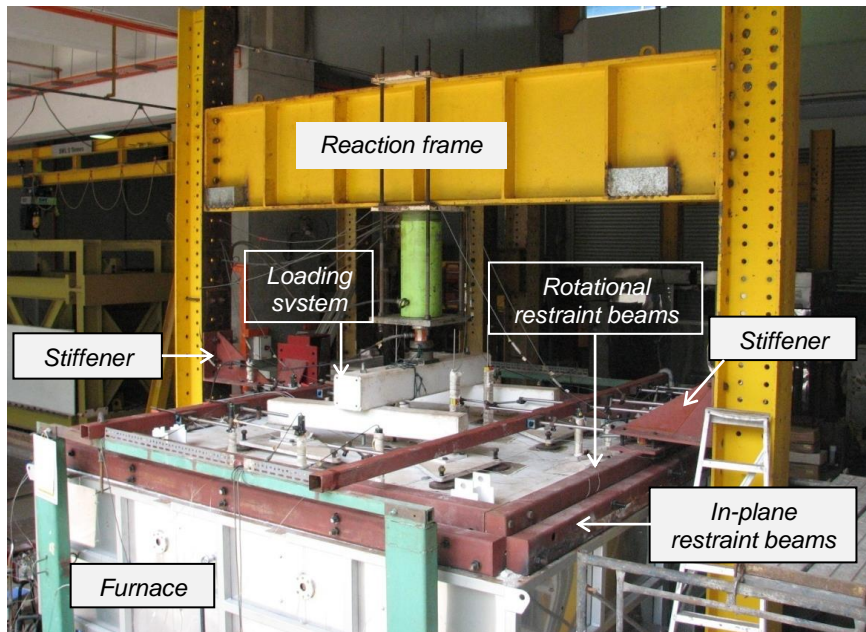


Fig. 10 Typical test setup

The tests were terminated when “failure” occurred. This was defined as the time when either:

- (1) Full-depth cracks with the crack width of about 10mm in the vicinity of the edge beams or failure of compression ring can be observed clearly; or
- (2) There was a significant drop in the mechanical resistance, and the hydraulic jack could no longer maintain the load level (violation of criterion “R”).

4.3.2 Comparison principles

Verification of deflection limits

Fig. 11 shows typical test results of a tested specimen in which temperatures of the slab (bottom and top surfaces, and reinforcing mesh) were indicated together with the deflection at the slab centre. The P288 deflection limit (Eq. (1)) was then calculated using the assumption that $(T_2 - T_1)$ is equal to 770°C for fire exposure below 90 minutes

and 900°C thereafter. T_2 and T_1 are the bottom and top surface temperatures of the slab respectively. Based on the temperatures measured at failure point, T_2 and T_1 were determined, and then the P390 deflection limit was calculated. Comparisons between these two deflection limits and test results are presented in **Section 4.3.3.1**.

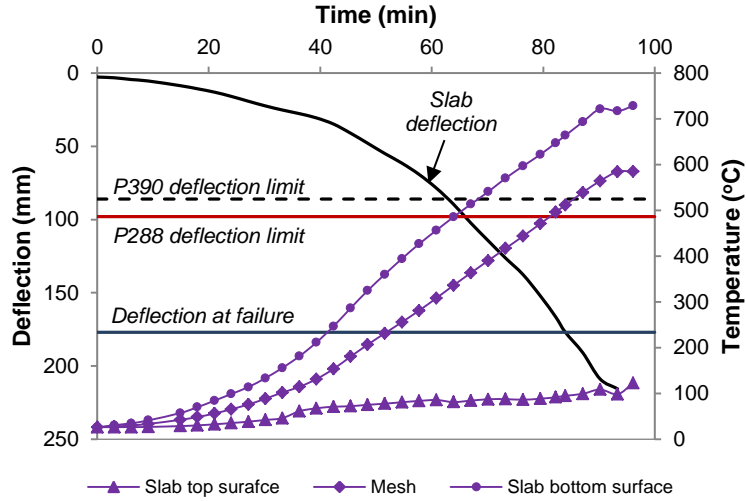


Fig. 11 Typical test results

Comparisons of load-bearing capacity for specimens without unprotected interior beams

Since the Bailey-BRE method does not explicitly consider the deflection of the edge beams, the enhancement factor predicted by P288 (e) is calculated using *the relative slab deflection* measured at failure and compared with the enhancement factor determined from the tests (e_{test}). To compare the predicted load-bearing capacity with test results, the deflection at failure of all specimens is used.

The relative slab deflection from the tests can be calculated by Eq. (2).

$$\text{Relative slab deflection: } w_r = w_m - \frac{1}{4}(w_{MB1} + w_{MB2} + w_{PSB1} + w_{PSB2}) \quad (2)$$

where w_{MB1} , w_{MB2} are the deflection of two main edge beams corresponding to w_m ;
 w_{PSB1} , w_{PSB2} are the deflection of two secondary edge beams corresponding to w_m .

For the specimens without unprotected interior beams, the comparison was straightforward. Based on the relative slab deflection Eq. (2), following the design procedure as in **Fig. 6**, the enhancement factor was calculated and compared with that determined from the tests. The load-bearing capacity of the beam-slab systems *without the interior beams* is equal to $e \times p_{y,\theta}$ ($p_{y,\theta}$ is the yield load at failure temperature).

Comparisons of load-bearing capacity for specimens with unprotected interior beams

The 4th assumption of the Bailey-BRE method is that the load-carrying capacity of *the composite unprotected interior beams* and the slab (enhanced due to TMA) are added together provided that the unprotected interior beams have not failed yet. The load-carrying capacity of the beam-slab floor systems *with the interior beams* can be calculated using Eq. (3).

$$q_{t,\theta} = e \times p_{y,\theta} + p_{b,\theta} \quad (3)$$

where $q_{t,\theta}$ is the total capacity of the slab at temperature θ ; e is the enhancement factor; $p_{y,\theta}$ is the yield load at temperature θ ; $p_{b,\theta}$ is the increase in the slab load capacity due to flexural strength of the unprotected interior beams at temperature θ if these beams have not failed.

The load-carrying capacity of *composite unprotected interior beam* refer to the bending moment resistance of the beam calculated by using I-steel section plus concrete flange on top of the steel section.

To check the 4th assumption of the Bailey-BRE method, when calculating part of the load supported by the unprotected interior beams, two cases are considered, viz. Case 1 – treating the interior beams as composite beams with part of concrete slab lying above the steel beam, and Case 2 – bare steel beam.

At the loading phase, the specimens with unprotected interior beams were loaded to a predetermined value. This load was kept constant and then temperature was increased up to failure. At failure, the test load would be supported by TMA mobilised in the slab

together with any residual flexural resistance of unprotected interior beams. Therefore, the steps used to validate the P288 against the specimens with interior beams are as follows:

- Check if the interior beams have failed yet using the bending moment capacity method in BS EN 1994-1-2 [6].
- If the beams had failed, the test load was totally resisted by the slab. The enhancement factor is calculated and compared with that determined from the test.
- If the interior beams had not failed yet, the load supported by the interior beams would be subtracted from the test load. The remainder load was used to calculate the actual enhancement factor and then compared to the predictions by P288.

4.3.3 Summary of comparison results

In this section, only a summary of comparison results is presented. Details can be found in **Appendix C**.

4.3.3.1 Deflection limits

Table 5 shows comparisons of the P288 and P390 deflection limits against the test results. It can be seen that all the specimens failed at a deflection greater than the P288 and P390 deflection limits. This indicates that the P288 deflection limit is conservative with the ratio of prediction-to-test deflection varying from 0.45 to 0.86. The deflection limit from P390 is even more conservative with the ratio of prediction-to-test deflection ranging from 0.40 to 0.75.

Table 5 Comparisons of deflection limits (P288 and P390) against test results

Series	Test	Slab depth	Deflection due to thermal curvature	Deflection due to mechanical strain	P288 deflection limit (Eq. (1))	P390 deflection limit	Max. deflection in test*	P288 / Test	P390 / Test
		mm	mm	mm	mm	mm	mm		
I	S1	55	44	54	98	80	131	0.75	0.61
	S2-FR-IB	55	44	54	98	86	177	0.55	0.49
	S3-FR	58	42	57	99	73	115	0.86	0.63
II	P215-M1099	57	43	57	99	84	124	0.80	0.68
	P368-M1099	58	42	57	99	88	118	0.84	0.74
	P486-M1099	55	52	57	108	90	139	0.78	0.65
	P215-M1356	58	42	57	99	91	121	0.81	0.75
	P215-M2110	59	48	57	105	83	143	0.74	0.58
	ISOCS3	60	25	52	86	77	178	0.48	0.43
III	ISOCS1	60	28	56	96	84	208	0.46	0.40
	ISOCS2	60	33	51	85	84	189	0.45	0.44
	ICS1	60	34	57	97	91	184	0.53	0.49
IV	ECS1	60	35	53	93	88	190	0.49	0.46
	CCS1	60	34	50	90	84	179	0.50	0.47
	ICS2	60	35	52	92	87	153	0.60	0.57
V	ECS2	60	35	50	90	85	158	0.57	0.54
	CCS2	60	36	51	91	87	160	0.57	0.54
M =								0.63	0.56

* Test terminated when fracture of reinforcement had been identified.

4.3.3.2 Load-bearing capacity

The comparisons shows that when calculating part of the load supported by the unprotected interior beams, if the interior beams are treated as bare steel beams, the method proposed in SCI P288 is conservative. As can be seen in **Tables 6 & 7**, P288 gives a smaller prediction compared to the test results (about 17% in average for Series I and II, 11% in average for Series III, IV and V).

Table 6 Comparison of P288 predictions against test results – Series I and II
(unprotected interior beams are treated as bare steel beams)

<i>Series</i>	<i>Test</i>	P_{test} <i>kN/m²</i>	<i>MB</i> <i>def.</i> <i>mm</i>	<i>PSB</i> <i>def.</i> <i>mm</i>	<i>Slab</i> <i>def.</i> <i>mm</i>	<i>Relative</i> <i>def.</i> <i>mm</i>	<i>Total capacity</i> <i>(kN/m²)</i> <i>(Eq. 2)</i>	<i>Prediction</i> <i>/ Test</i> <i>(Eq. 2)</i>
<i>I</i>	<i>S1</i>	15.6	28	58	131	88	13.1	0.84
	<i>S2-FR-IB</i>	15.1	56	84	177	107	10.4	0.69
	<i>S3-FR</i>	16.0	33	28	115	85	14.6	0.92
							<i>M =</i>	0.82
<i>II</i>	<i>P215-M1099</i>	15.6	38	57	124	76	14.2	0.91
	<i>P368-M1099</i>	15.3	51	83	118	51	11.9	0.78
	<i>P486-M1099</i>	15.5	55	94	139	64	12.9	0.83
	<i>P215-M1356</i>	15.4	59	88	121	48	12.2	0.79
	<i>P215-M2110</i>	15.6	39	79	143	84	13.1	0.84
							<i>M =</i>	0.83

Table 7 Comparison of P288 predictions against test results – Series III, IV and V
(unprotected interior beams are treated as bare steel beams)

<i>Series</i>	<i>Specimen</i>	P_{test} <i>kN/m²</i>	$P_{y,\theta}$ <i>kN/m²</i>	<i>Slab</i> <i>deflection</i> w_m <i>mm</i>	<i>Average</i> <i>beam</i> <i>defl.</i> <i>mm</i>	<i>Relative</i> <i>slab</i> <i>deflection</i> <i>mm</i>	<i>Enhance</i> <i>ment</i> <i>factor e</i>	<i>Total</i> <i>capacity</i> $eP_{y,\theta}$ <i>kN/m²</i>	<i>Prediction</i> <i>/ Test</i>
<i>III</i>	ISOCS3	20	9.94	178	83	95	1.84	18.3	0.91
	ISOCS1	20	7.89	208	80	128	2.16	17.1	0.85
	ISOCS2	30	19.25	189	130	59	1.40	27.0	0.90
							<i>M =</i>	0.89	
<i>IV</i>	ICS1	20	7.06	184	24	140	2.29	16.1	0.81
	ECS1	20	8.72	190	58	122	2.10	18.3	0.91
	CCS1	20	9.5	179	81	98	1.86	17.7	0.88
							<i>M =</i>	0.87	
<i>IV</i>	ICS2	30	17.48	153	68	85	1.61	28.0	0.93
	ECS2	30	17.97	158	83	75	1.54	27.6	0.92
	CCS2	30	19.21	160	91	69	1.47	28.2	0.94
							<i>M =</i>	0.93	

Therefore, it can be concluded that SCI P288 and P390 are conservative provided that: (1) when calculating the slab enhancement factor, *the deflection limit proposed in SCI P288 & P390* is used; (2) when calculating the total load-bearing capacity of the beam-slab floor system, the unprotected interior beams are treated as *steel beams*. However, *since the residual capacity of unprotected interior beams under fire conditions is very small, it is recommended to ignore this capacity*.

4.4 Conclusions

In **Section 4**, a summary of fire test results conducted in NTU is presented. The comparisons between the P288 and P390 predictions against the test results are conducted. The following points can be drawn:

(1) *The Bailey-BRE method*

SCI P288 and P390 are conservative provided that: (1) when calculating the slab enhancement factor, *the deflection limit proposed in SCI P288 or P390* is used; (2) when calculating the total load-bearing capacity of beam-slab floor systems, the unprotected interior beams is ignored.

(2) *Design procedure*

As discussed above, the comparisons between the predicted results by the Bailey-BRE method and the test results conducted by NTU show that the Bailey-BRE method is conservative provided that the unprotected interior beams are treated as *bare steel beams*. However, since the residual capacity of unprotected interior beams under fire conditions is very small, this capacity can be ignored.

Therefore, the following point in the design procedure (**Fig. 6**) should be revised as follows:

*“The load carrying capacity of **the unprotected interior steel beams** under fire conditions is ignored”.*

The revised design procedure is shown in **Fig. 12**.

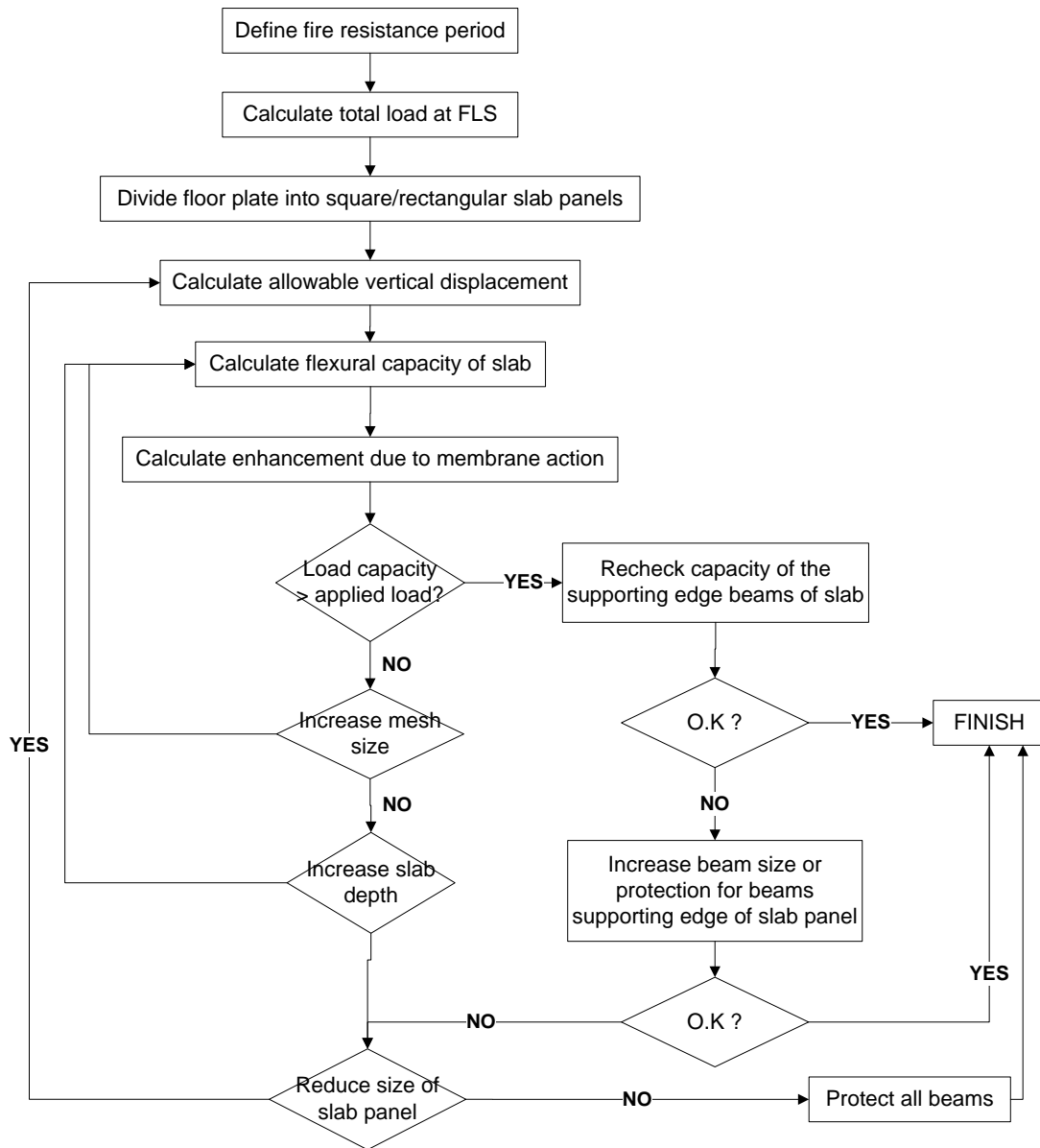


Fig. 12 Revised design procedure of the Bailey-BRE method

5 CONCLUSIONS

This design commentary provides discussions on each section of SCI Publications P288 and P390 which are based on the Bailey-BRE method to design composite floor steel-framed buildings. This method allows interior secondary beams to be unprotected so that fire-protection costs can be reduced.

Based on the calibration of the Bailey-BRE method against five test series (17 composite beam-slab floor system specimens in total) tested under fire conditions in NTU, it is concluded that the Bailey-BRE method is conservative and SCI P288 and P390 can be used with the following conditions:

- (1) When calculating the slab enhancement factor, *the deflection limit proposed in SCI P288& P390* is used;
- (2) The load carrying capacity of the unprotected interior steel beams under fire conditions is ignored.
- (3) The required bending moment resistance of the edge beams must be checked by considering alternative yield line patterns that would allow the slab to fold along an axis of symmetry without developing TMA. Details of the calculation method are given in Section 2 of SCI P390. This procedure shall be followed.
- (4) When TMA is mobilised, the secondary and main fire-protected edge beams carry more load at the fire limit state. Therefore, the load ratios of the beams increase. This must be considered when determining the critical temperature for the beams and appropriate levels of fire protection.

The SCI Publications P288 and P390 and this commentary shall not be used to replace SS EN 1994-1-1:2004 and SS EN 1994-1-2:2005 in the design of composite steel-frame buildings under fire conditions. They only provide design guidance on an advanced calculation method that engineers may use in the design of composite steel-framed buildings. In addition, all the detailing clauses in SS EN 1994-1-1:2004 at ambient design such as anchoring for steel mesh, shear stud design, stud spacing, etc. shall be complied.

References

- [1] EN 1994-1-1: *Eurocode 4. Design of Composite Steel and Concrete Structures. Part 1-1: General Rules and Rules for Buildings*. European Committee for Standardization (CEN), Brussels, Belgium, 2004.
- [2] EN 1994-1-2: *Eurocode 4. Design of composite steel and concrete structures - Part 1-2: General Rules - Structural fire design*. European Committee for Standardization (CEN), Brussels, Belgium, 2005.
- [3] Newman GM, Robinson JT, Bailey CG. *Fire Safe Design: A new Approach to Multi-Story Steel-Framed Buildings*. Technical Report. 2nd: The Steel Construction Institute. SCI Publication P288. 2006.
- [4] Simms WI, Bake S. *TSLAB V3.0 User Guidance and Engineering Update*. The Steel Construction Institute. SCI Publication P390. 2010.
- [5] EN 1991-1-2: *Eurocode 1. Actions on structures - Part 1-2: General actions - Actions on structures exposed to fire*. European Committee for Standardization (CEN), Brussels, Belgium, 2002.
- [6] EN 1990: *Eurocode 0. Basis of structural design*. European Committee for Standardization (CEN) Brussels, Belgium, 2002.
- [7] Bailey CG, Toh WS. Small-scale concrete slab tests at ambient and elevated temperatures. *Engineering Structures*. 2007;29:2775-91.
- [8] Foster SJ, Bailey CG, Burgess IW, Plank RJ. Experimental behaviour of concrete floor slabs at large displacements. *Engineering Structures*. 2004;26:1231-47.
- [9] Tan KH, Nguyen TT, Liu JX. *Explore Concept of Membrane Action in Slabs to Reduce Fire Protection for Beams*. Project report. Nanyang Technological University, School of Civil and Environmental Engineering. 2013.

- [10] NA to SS EN 1994-1-2: *Singapore National Annex to Eurocode 4. Design of composite steel and concrete structures. Part 1-2: General rules - Structural fire design*. SPRING Singapore, Singapore, 2009.
- [11] Francis P, Simms I. *NCCI - Fire resistance design of composite slabs*. The Steel Construction Institute. Eurocodes Non Contradictory Complementary Information (NCCI). 2012.
- [12] EN 1993-1-8: *Eurocode 3. Design of Steel Structures - Part 1-8: Design of joints*. European Committee for Standardization (CEN), Brussels, Belgium, 2005.
- [13] Nunez E. *NCCI Initial sizing of simple end plate connections*. Technical Report SN013a. The Steel Construction Institute. Eurocodes Non Contradictory Complementary Information (NCCI). 2005a.
- [14] Nunez E. *NCCI Initial sizing of fin plate connections*. Technical Report SN016a. The Steel Construction Institute. Eurocodes Non Contradictory Complementary Information (NCCI). 2005b.
- [15] Bailey CG, Moore DB. Structural behaviour of steel frames with composite floorslabs subject to fire: Part 1: Theory. *Structural engineer London*. 2000a;78:19-27.
- [16] Zhao B, Roosefid M, Vassart O. Full scale test of a steel and concrete composite floor exposed to ISO fire. Proceedings of the Fifth International Conference on Structures in Fire (SiF'08). Singapore. Nanyang Technological University; 2008. p. 539-50.
- [17] Bailey CG, Moore DB. Structural behaviour of steel frames with composite floorslabs subject to fire: Part 2: Design. *Structural engineer London*. 2000b;78:28-33.

[18] Bailey CG, Lennon T, Moore DB. Behaviour of full-scale steel-framed buildings subjected to compartment fires. *Structural engineer London*. 1999;77:15-21.

[19] Bailey CG, Toh WS. Behaviour of concrete floor slabs at ambient and elevated temperatures. *Fire Safety Journal*. 2007;42:425-36.

[20] BS 5950-8: *Structural use of steelwork in building. Part 8: Code of practice for fire resistant design*. British Standard Institution (BSI), London, 2003.

APPENDIX A THE BAILEY-BRE METHOD

(Bailey and Moore 2000; Bailey 2003; Bailey and Toh 2007)

This Appendix summarizes the Bailey-BRE method for reference only. More details can be found in Bailey and Moore (2000a; 2000b), Bailey (2003), Bailey and Toh (2007).

The load bearing capacity of a two-way spanning simply supported slab, with no in-plane horizontal restraint at its edges, is greater than that calculated using the conventional yield-line theory. The load capacity is enhanced by tensile membrane action mobilised in the slab at large displacement and by the increase of the yield moment in the outer regions of the slab, where compressive stresses occur across the yield lines (see **Fig. A2**).

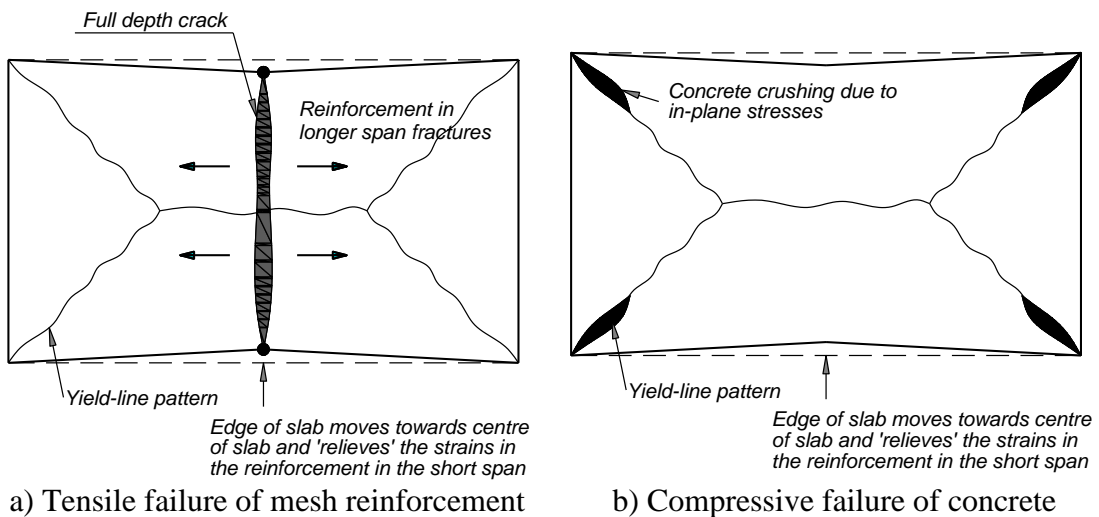


Fig. A1 Assumed failure modes for composite floor

It is assumed that at ultimate conditions the yield line pattern will be as shown in **Fig. A1(a)** and that failure will occur due to fracture of the mesh across the short span at the centre of the slab. A second mode of failure might, in some cases, occur due to crushing of the concrete in the corners of the slab where high compressive in-plane forces occur as shown by **Fig. A1(b)**. This mode of failure is discussed in the end of this Appendix.

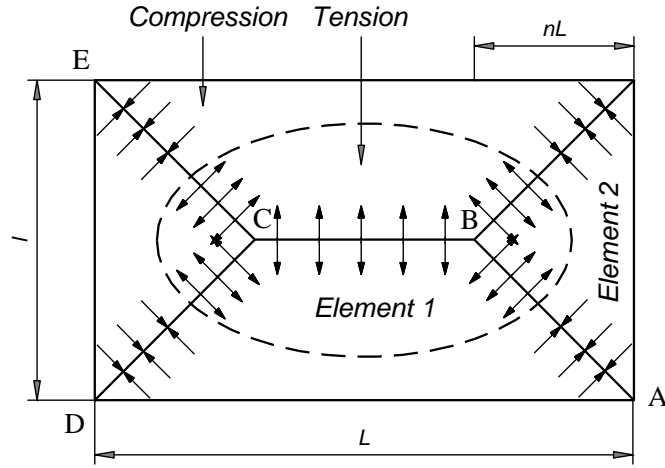


Fig. A2 Rectangular slab simply supported on four edges showing in-plane forces across the yield lines due to TMA

Fig. A2 shows a rectangular simply supported slab and the lower bound yield-line pattern subjected to uniformly distributed loading. The intersection of the yield lines is defined by the parameter n which is given by:

$$n = \frac{1}{2\sqrt{\mu a^2}} \left[\sqrt{3\mu a^2 + 1} - 1 \right] \leq 0.5$$

n is limited to maximum of 0.5 resulting in a valid yield line pattern; a is the aspect ratio of the slab (L/l); μ is the ratio of the yield moment capacity of the slab in orthogonal directions ($\mu \leq 1.0$).

The yield line load of the slab based on the formation of these yield lines is given by:

$$p_y = \frac{24\mu M_0}{l^2} \left[\sqrt{3 + \frac{1}{(\sqrt{\mu a})^2} - \frac{1}{\sqrt{\mu a}}} \right]^{-2}$$

Hayes (1968a) noted that assuming rigid-plastic behaviour, only rigid body translations and rotations are allowed. Further assumptions that the neutral axes along the yield lines are straight lines and that the concrete stress-block is rectangular. It means that the variations in membrane forces along the yield lines become linear (**Fig. A3**). These assumptions and the resulting distribution of membrane forces were also adopted by Bailey.

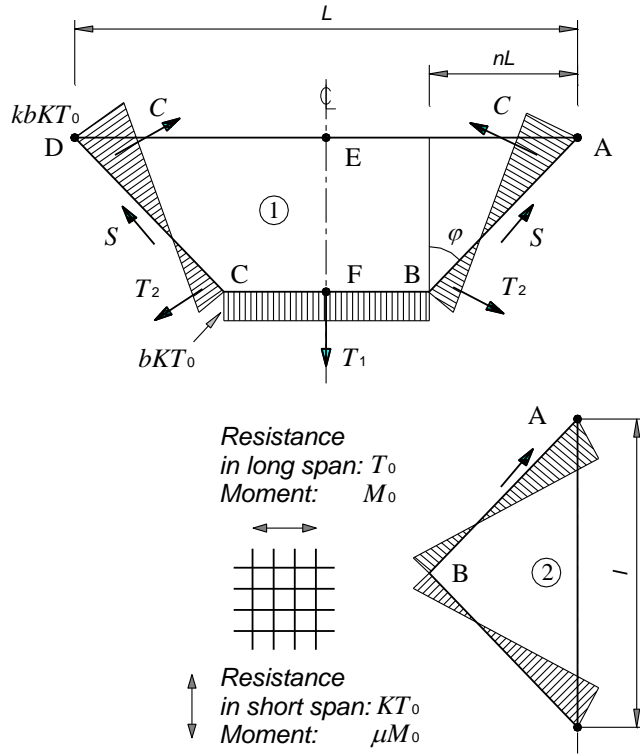


Fig. A3 In-plane stress distribution for the elements 1 and 2

Derivation of an expression for parameter k

Considering the equilibrium of the in-plane forces T_1 , T_2 and C acting on Element 1 allows the following relationships to be derived, where ϕ is the angle defining the yield line pattern.

$$\frac{T_1}{2} \sin \phi = C - T_2 \tag{A.1}$$

$$x = \frac{L}{2} \cos \phi - \frac{L/2 - nL}{\cos \phi}; \quad y = \frac{1}{1+k} \sqrt{(nL)^2 + \frac{l^2}{4}}$$

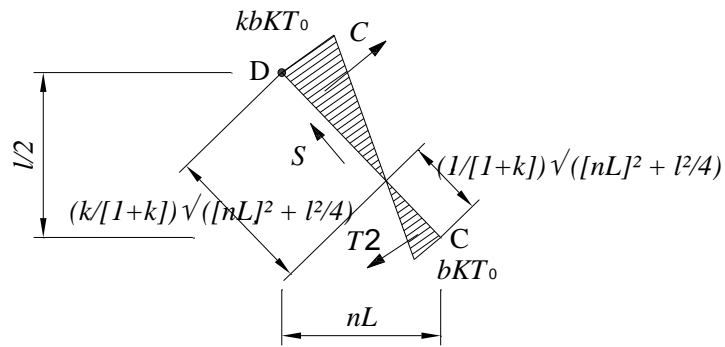


Fig. A4 In-plane stress distribution along yield line CD

Fig. A4 shows the geometry of the stress distribution along yield line CD. From **Figs. A.3** and **A.4**, one can have:

$$\begin{aligned}
 T_1 &= bKT_0(L - 2nL) \\
 T_2 &= \frac{bKT_0}{2} \left(\frac{1}{1+k} \right) \sqrt{(nL)^2 + \frac{l^2}{4}} \\
 C &= \frac{kbKT_0}{2} \left(\frac{k}{1+k} \right) \sqrt{(nL)^2 + \frac{l^2}{4}} \\
 \sin \varphi &= \frac{nL}{\sqrt{(nL)^2 + \frac{l^2}{4}}}
 \end{aligned}$$

Substituting the above expressions into Eq. (A.1) gives:

$$\frac{bKT_0(L - 2nL)}{2} \frac{nL}{\sqrt{(nL)^2 + \frac{l^2}{4}}} = \frac{kbKT_0}{2} \left(\frac{k}{1+k} \right) \sqrt{(nL)^2 + \frac{l^2}{4}} - \frac{bKT_0}{2} \left(\frac{1}{1+k} \right) \sqrt{(nL)^2 + \frac{l^2}{4}}$$

This gives:

$$k = \frac{4na^2(1 - 2n)}{4n^2a^2 + 1} + 1 \tag{A.2}$$

Derivation of an expression for parameter b

Considering the fracture of the reinforcement across the short span of the slab, an expression for the parameter b can be obtained. The line EF shown in **Fig. A5** represents the location of the mesh fracture, which will result in a full depth crack across the slab. An upper bound solution for the in-plane moment of resistance along the line EF can be obtained by assuming that all the reinforcement along the section is at ultimate stress (f_u) and the centroid of the compressive stress block is at location E in **Fig. A5**. It is assumed that:

$$f_u = 1.1f_y$$

where f_y is the yield stress.

$$C = \frac{l^2}{16n}(k-1)$$

$$D = \left(\frac{L}{2} - nL\right)\left(\frac{L}{4} - \frac{nL}{2}\right)$$

Membrane forces

The load bearing capacity for Elements 1 and 2 of the slab can be determined by considering the contribution of the membrane forces to the resistance and the increase in bending resistance across the yield lines separately. These effects are expressed in terms of an enhancement factor, to be applied to the lower bound yield line resistance. The effect of the inplane shear S (**Fig. A3**) or any vertical shear on the yield line was initially ignored, resulting in two unequal loads being calculated for Elements 1 and 2 respectively. An averaged value was then calculated, considering contribution of the shear forces.

Contribution of membrane forces to load bearing capacity

a) Element 1

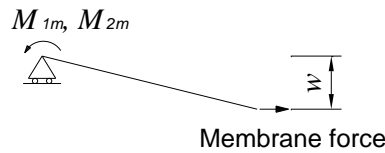


Fig. A6 Calculating the moment caused by the membrane force

We have:

$$M_{1m} = KT_0 Lbw \left((1-2n) + \frac{n(3k+2)}{3(1+k)^2} - \frac{nk^3}{3(1+k)^2} \right)$$

where M_{1m} is the moment about the support due to membrane forces for element 1.

The above formulation defines the contribution from the membrane forces to the load bearing capacity that needs to be added to the contribution due to the enhanced bending capacity in the areas where the slab is experiencing compression forces. For simplicity, the contribution from the membrane forces and enhanced bending action is related to the normal yield line load. This allows an enhancement factor to be

calculated for both the membrane force and the enhanced bending moments. These enhancement factors can finally be added to give the overall enhancement of the slab due to membrane action. Dividing M_{1m} by $\mu M_o L$, the resistance moment of the slab, when no axial force is present, allows the effect of TMA to be expressed as an enhancement of yield line resistance. The value of $\mu M_o L$ is obtained based on **Fig. A7**.

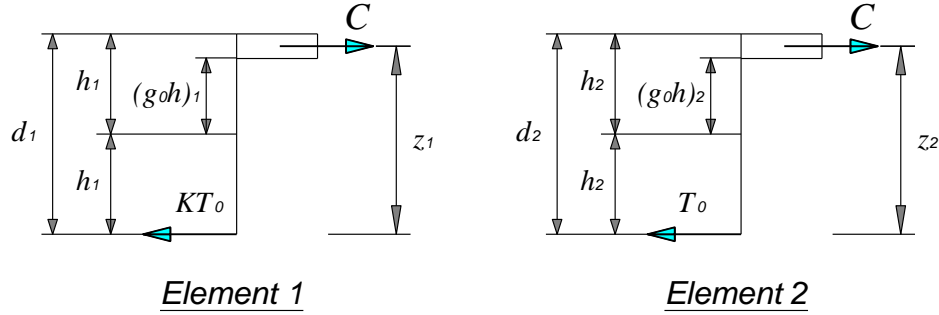


Fig. A7 Calculation of the moment resistance

The bending moments μM_o and M_o per unit width of slab in each orthogonal direction are given by:

$$\mu M_o = KT_o z_1 = KT_o d_1 \left(\frac{3 + (g_o)_1}{4} \right)$$

$$M_o = T_o z_2 = T_o d_2 \left(\frac{3 + (g_o)_2}{4} \right)$$

where $(g_o)_1$ and $(g_o)_2$ are parameters which define the flexural stress block in short and long spans, respectively.

The enhancement factor, e_{1m} , is given by:

$$e_{1m} = \frac{M_{1m}}{\mu M_o L} = \frac{4b}{3 + (g_o)_1} \left(\frac{w}{d_1} \right) \left((1 - 2n) + \frac{n(3k + 2)}{3(1 + k)^2} - \frac{nk^3}{3(1 + k)^2} \right) \quad (\text{A.4})$$

b) *Element 2*

The moment about the support due to the membrane forces is given by:

$$M_{2m} = KT_o lbw \left(\frac{2 + 3k}{6(1 + k)^2} - \frac{k^3}{6(1 + k)^2} \right)$$

The effect of tensile membrane action can be expressed as an enhancement of yield line resistance by dividing the moment about the support due to membrane action, M_{2m} by the moment resistance in the longitudinal direction, when no axial force is present, $M_o l$, which results in:

$$e_{2m} = \frac{M_{2m}}{M_o l} = \frac{4bK}{3+(g_o)_2} \left(\frac{w}{d_2} \right) \left(\frac{2+3k}{6(1+k)^2} - \frac{k^3}{6(1+k)^2} \right) \quad (\text{A.5})$$

The effect of the membrane forces on the bending resistance along the yield lines is evaluated by considering the yield criterion when axial load is also present, as given by Wood (1961). In the case of the short span the bending moment in the presence of an axial force is given by:

$$\frac{M_N}{\mu M_o} = 1 + \alpha_1 \left(\frac{N}{KT_o} \right) - \beta_1 \left(\frac{N}{KT_o} \right)^2 \quad (\text{A.6})$$

where:

$$\alpha_1 = \frac{2(g_o)_1}{3+(g_o)_1}; \beta_1 = \frac{1-(g_o)_1}{3+(g_o)_1}$$

Similarly for the long span,

$$\frac{M_N}{M_o} = 1 + \alpha_2 \left(\frac{N}{T_o} \right) - \beta_2 \left(\frac{N}{T_o} \right)^2 \quad (\text{A.7})$$

where:

$$\alpha_2 = \frac{2(g_o)_2}{3+(g_o)_2}; \beta_2 = \frac{1-(g_o)_2}{3+(g_o)_2}$$

Effect of membrane forces on bending resistance

a) Element 1

The effect of the membrane forces on the bending resistance is considered separately for each yield line. Along the yield line BC:

$$\left(\frac{M_N}{M_0}\right)_{BC} = 1 - \alpha_1 b - \beta_1 b^2$$

Along the yield line AB, the membrane force across the yield line, at a distance of x from B is given by:

$$N_x = -bKT_0 + \frac{x}{nL}(k+1)bKT_0 = bKT_0\left(\frac{x}{nL}(k+1) - 1\right)$$

Substitution into Eq. (A.6) gives, for yield lines AB and CD:

$$2 \int_0^{nL} \frac{M}{M_0} dx = 2nL \left[1 + \frac{\alpha_1 b}{2}(k-1) - \frac{\beta_1 b^2}{3}(k^2 - k + 1) \right]$$

The enhancement of bending resistance due to membrane forces on Element 1 is given by:

$$e_{1b} = \frac{M}{\mu M_0 L} = 2n \left[1 + \frac{\alpha_1 b}{2}(k-1) - \frac{\beta_1 b^2}{3}(k^2 - k + 1) \right] + (1-2n)(1 - \alpha_1 b - \beta_1 b^2) \quad (\text{A.8})$$

b) *Element 2*

Referring to **Fig. A8** for element 2, the force at a distance y from B can be expressed as:

$$N_y = -bKT_0 + \frac{y}{l/2}(k+1)bKT_0 = bKT_0\left(\frac{2y}{l}(k+1) - 1\right)$$

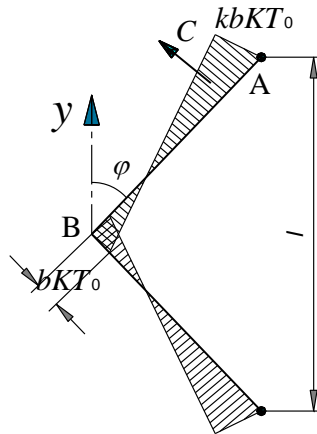


Fig. A8 Forces applied to element 2

Resulting in,

$$2 \int_0^{l/2} \frac{M}{M_0} dx = l \left[1 + \frac{\alpha_2 b}{2} (k-1) - \frac{\beta_2 b^2}{3} (k^2 - k + 1) \right]$$

which gives the enhancement factor due to the effect of the membrane forces on the bending resistance according to the following formulation:

$$e_{2b} = \frac{M}{M_0 l} = 1 + \frac{\alpha_2 b K}{2} (k-1) - \frac{\beta_2 b^2 K}{3} (k^2 - k + 1) \quad (\text{A.9})$$

Combined enhancement factor for each element

Eqs. (A.4), (A.5), (A.8) and (A.9) provide the contribution to the load bearing capacity due to the membrane forces and the effect of the membrane forces on the bending resistance of the slab. Consequently, the combined enhancement factor is obtained for each element as follows:

$$\begin{aligned} e_1 &= e_{1m} + e_{1b} \\ e_2 &= e_{2m} + e_{2b} \end{aligned}$$

As stated earlier, the values e_1 and e_2 calculated based on the equilibrium of elements 1 and 2 will not be the same and Hayes (1968a) suggests that these differences can be explained by the effect of the vertical or in-plane shear and that the overall enhancement is given by:

$$e = e_1 - \frac{e_1 - e_2}{1 + 2\mu a^2}$$

Compressive failure of concrete

The abovementioned enhancement factor was derived by considering tensile failure of the mesh reinforcement. However, compressive failure of the concrete in the proximity of the slab corners must also be considered as a possible mode of failure, which in some cases may precede mesh fracture. This was achieved by limiting the value of the parameter ‘ b ’, which represents the magnitude of the in-plane stresses.

According to **Fig. A3**, the maximum in-plane compressive force at the corners of the slab is given by $kbKT_0$. The compressive force due to bending should also be considered. By assuming that the maximum stress-block depth is limited to $0.45d$, and adopting an average effective depth to the reinforcement in both orthogonal directions results in:

$$kbKT_0 + \left(\frac{KT_0 + T_0}{2} \right) = 0.85f_{ck} \times 0.45 \left(\frac{d_1 + d_2}{2} \right)$$

where f_{ck} is the concrete cylinder strength.

Solving for the constant b gives:

$$b = \frac{1}{kKT_0} \left[0.85f_{ck} \cdot 0.45 \left(\frac{d_1 + d_2}{2} \right) - T_0 \left(\frac{K+1}{2} \right) \right] \quad (\text{A.10})$$

The constant b is then taken as the minimum value given by the Eqs. (A.3) and (A.10).

Reference

- Bailey, C. G. (2003). "Efficient arrangement of reinforcement for membrane behaviour of composite floor slabs in fire conditions". *Journal of Constructional Steel Research*, 59(7), 931-949.
- Bailey, C. G. and Moore, D. B. (2000a). "Structural behaviour of steel frames with composite floorslabs subject to fire: Part 1: Theory". *Structural engineer London*, 78(Compendex), 19-27.
- Bailey, C. G. and Moore, D. B. (2000b). "Structural behaviour of steel frames with composite floorslabs subject to fire: Part 2: Design". *Structural engineer London*, 78(Compendex), 28-33.
- Bailey, C. G. and Toh, W. S. (2007). "Behaviour of concrete floor slabs at ambient and elevated temperatures". *Fire Safety Journal*, 42(6-7), 425-436.
- Hayes, B. (1968a). "Allowing for membrane action in plastic analysis of rectangular reinforced concrete slabs". *Magazine of Concrete Research*, 20(65), 205-212.
- Wood, R. H. (1961). *Plastic and elastic design of slabs and plates*. New York, Ronald Press Co. 344p.

**APPENDIX B ESTIMATION OF COST SAVING OF FIRE PROTECTION
FOR A TYPICAL COMPOSITE FLOOR BY USING SCI P288**

This Appendix presents an estimation of saving of fire protection cost for a typical composite floor by using SCI P288 [1] instead of using EN 1994-1-2 [2].

Fig. A1 shows the arrangement of steelwork at a typical floor level. The floor includes four by three bays with a total area of 1080 m². The floor plate for each storey consists of a composite floor slab constructed using Kingspan MD60 trapezoidal metal decking, normal weight concrete and a single layer of mesh reinforcement. The beams are designed in accordance with BS EN 1993-1-1 and BS EN 1994-1-1 [3, 4].

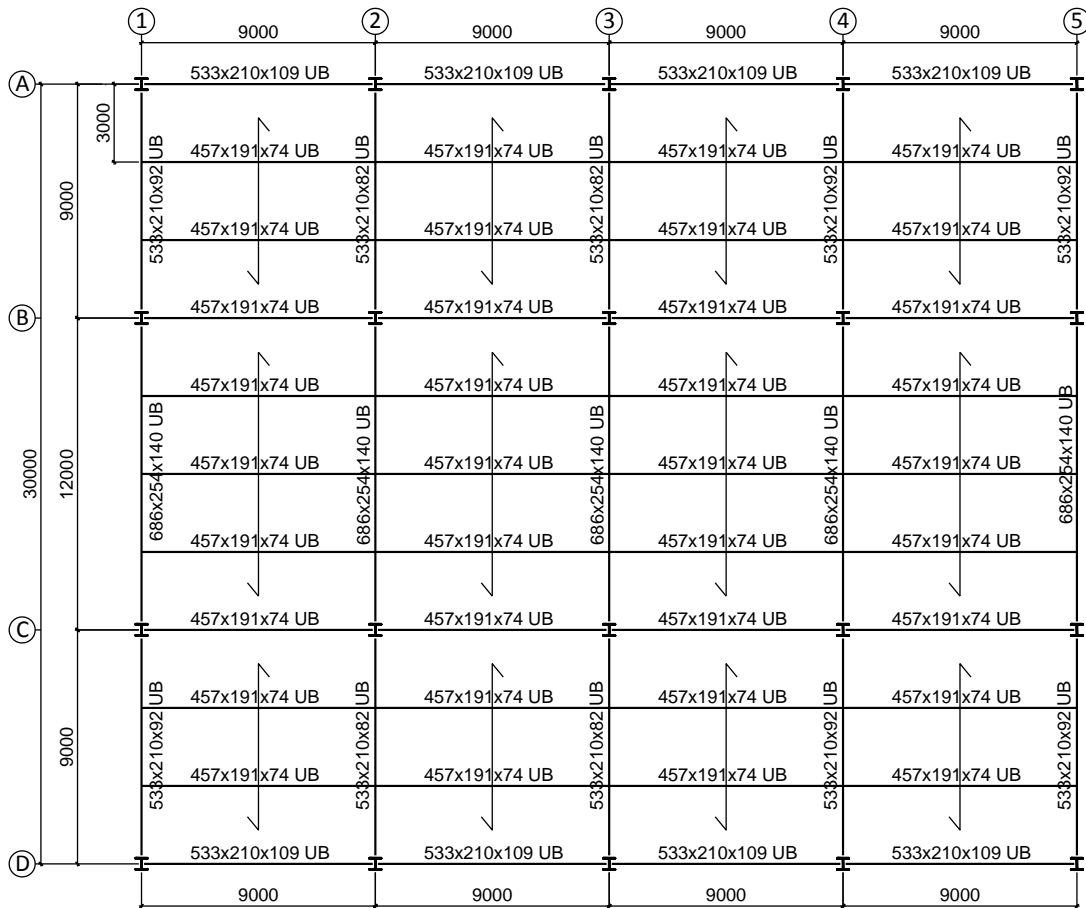


Fig. B1 Arrangement of steelwork at a typical floor level

The floor loading considered was as follows:

- Variable action: 4 kN/m²
- Variable action due to partitions: 1 kN/m²
- Permanent action due to ceilings and services: 0.7 kN/m²
- Self weight of beam: 0.5 kN/m²

For the edge beams, an additional cladding load of 2 kN/m was considered in their design. After the design at ambient temperature, the beam sizes required to satisfy the normal stage conditions (ultimate and serviceability limit states) for these actions are shown in **Fig. A1**. The internal beams are composite and the degree of shear connection for each beam is shown in Table 3.

Table B8 Beam details

<i>Beam (S355)</i>	<i>Location of beam</i>	<i>Construction type</i>	<i>Degree of shear connection (%)</i>	<i>Number of shear studs per group and spacing</i>
457x191x74 UKB	Secondary internal beam	Composite	54	1 @ 323 mm
533x210x109 UKB	Secondary edge beam	Non composite	n.a	
533x210x82 UKB	Main internal beam	Composite	96	2 @ 323 mm
533x210x92 UKB	Main edge beam	Non composite	n.a	
686x254x140 UKB	Main internal beam	Composite	100	2 @ 323 mm
686x254x140 UKB	Main edge beam	Non composite	n.a	

According to EN 1993-1-2, EN 1994-1-2 [2, 5], all the steel beams (secondary internal and edge beams, primary internal and edge beams) are needed to be fire-protected under a required fire resistance time, for example 90 minutes. If using SCI Publication P288 and P390, all secondary and main beams connected directly to the columns can be left unprotected as shown in **Fig. B2**.



Fig. B2 Fire-protected and unprotected beams in a typical floor level

The estimation of cost saving of fire protection of the composite floor is presented in **Table B9**. According to EN 1994-1-2, all the steel beams must be checked so that their flexural resistance is greater than bending design moment during a required fire resistance time, resulting in a need of fire protection for all beams. Therefore, the total length of fire-protected beams in accordance with EN 1994-1-2 is 546 m.

According to P288 and P390, the load-bearing capacity of the slab will increase by mobilizing tensile membrane action. Therefore, all interior secondary beams do not need to be fire-protected. The total length of fire-protected beams in accordance with P288 is 294 m. The percentage of cost saving is:

$$s = \frac{(546 - 294)}{546} = 46\%$$

Table B9 Estimation of cost saving of fire protection

<i>Beam (S355)</i>	<i>Location of beam</i>	<i>Number of beam</i>	<i>Length of a beam (m)</i>	<i>Total length (m)</i>	<i>Fire-protected</i>
457x191x74 UB	Secondary protected internal beam	8	9.0	72	Y
457x191x74 UB	Secondary unprotected interior beam	28	9.0	252	N
533x210x109 UB	Secondary protected edge beam	8	9.0	72	Y
533x210x82 UB	Main protected internal beam	6	9.0	54	Y
533x210x92 UB	Main protected edge beam	4	9.0	36	Y
686x254x140 UB	Main protected internal beam	3	12.0	36	Y
686x254x140 UB	Main protected edge beam	2	12.0	24	Y

Total length of fire-protected beams (P288): 294 m

Total length of fire-protected beams (EN 1994-1-2): 546 m

Percentage: **46%**

References

[1] Newman GM, Robinson JT, Bailey CG. *Fire Safe Design: A new Approach to Multi-Story Steel-Framed Buildings*. Technical Report. 2nd: The Steel Construction Institute. SCI Publication P288. 2006.

[2] EN 1994-1-2: *Eurocode 4. Design of composite steel and concrete structures - Part 1-2: General Rules - Structural fire design*. European Committee for Standardization (CEN), Brussels, Belgium, 2005.

[3] EN 1993-1-1: *Eurocode 3. Design of Steel Structures - Part 1-1: General Rules and Rules for Buildings*. European Committee for Standardization (CEN), Brussels, Belgium, 2005.

[4] EN 1994-1-1: *Eurocode 4. Design of Composite Steel and Concrete Structures. Part 1-1: General Rules and Rules for Buildings*. European Committee for Standardization (CEN), Brussels, Belgium, 2004.

[5] EN 1993-1-2: *Eurocode 3. Design of Steel Structures - Part 1-2: General Rules - Structural fire design*. European Committee for Standardization (CEN), Brussels, Belgium, 2005.

APPENDIX C CALIBRATION OF P288 AGAINST THE FIRE TESTS CONDUCTED IN NANYANG TECHNOLOGICAL UNIVERSITY (2010 – 2012)

1. Calibration of the Bailey-BRE method against test series I and II

1.1 Test series I & II

The first two series included eight specimens which were tested under fire condition to study the development of tensile membrane action (TMA) in composite beam-slab systems. Only brief information and results of these series are provided below so that the calibration of the simple design method can be conducted. Details of the test results and discussions can be found in [1, 2].

1.2 Test specimens

Test series I and II can be divided into two groups. *Group 1* consisted of two specimens, namely, S1 and S3-FR, which had no interior beams (**Fig. 3**). *Group 2* consisted of six specimens which had two interior beams (**Fig. 4**).

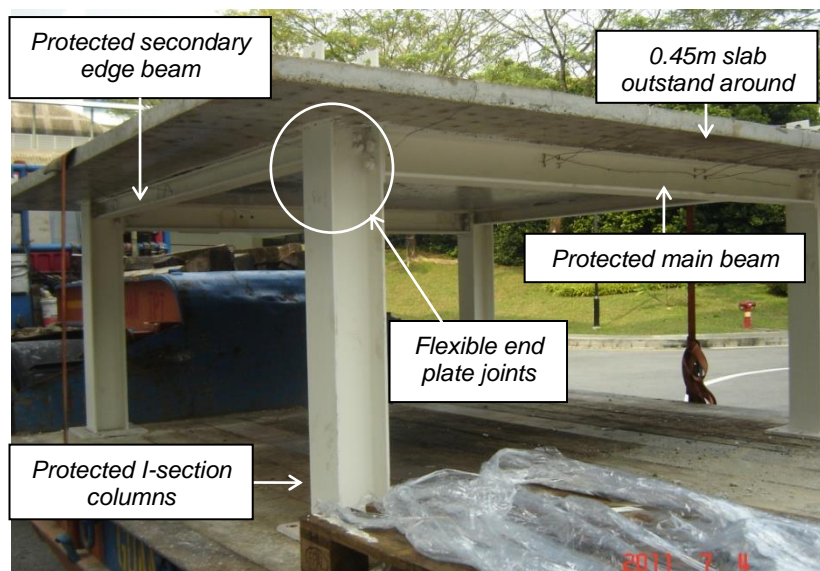


Fig. 3 Typical specimen without interior beams (S1 and S3-FR)

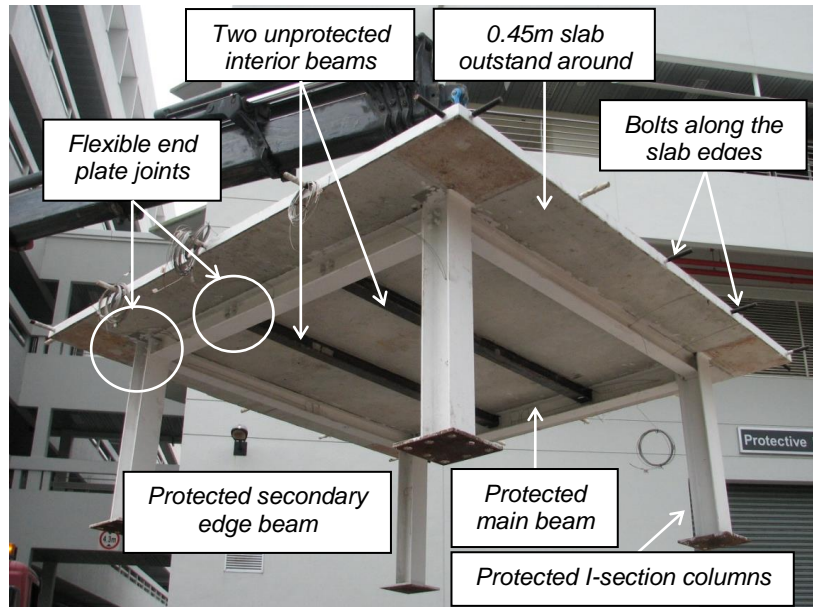


Fig. 4 Typical specimen with two unprotected interior beams

The specimens were of *one-quarter scale* due to limitations of laboratory facility and space. The slabs were 2.25m long and 2.25m wide with an overhang of 0.45m around all four edges, resulting in an aspect ratio of 1.0. Shrinkage reinforcement mesh with a grid size of 80mm x 80mm and a diameter of 3mm (giving a reinforcement ratio of 0.16%) was placed at about 38mm below the slab top surface. This concrete cover was ensured by 40mm x 40mm concrete spacers, placed at a grid of 320mm x 320mm. The 0.16% reinforcement ratio is close to the minimum value required by EN 1994-1-1 (0.2% for un-propped construction). The mesh was continuous across the whole slab, with no lapping of mesh. The specimens were cast using ready-mixed concrete, with the aggregate size ranging from 5 to 10mm, to enable adequate compaction during placement.

All the specimens were designed at elevated temperatures by using the fire protection strategy for members recommended in the SCI Publication P288. Therefore, all the edge beams and the columns were protected to a prescriptive one-hour fire-protection rating. No fire-proofing material was applied to the interior beams and the underside of the slabs.

Due to the 1:4 scaling there was no standard steel decking suitable for the slabs. To protect the heating elements from concrete spalling, the slabs were cast onto a 2mm thick steel sheet with small pre-drilled holes. The contribution of this sheet to the slab's load-bearing capacity was ignored, since the unprotected sheet would de-bond from the concrete slab, as observed in previous studies. The properties of the concrete slabs of all specimens are summarised in **Table 10**.

Table 10 Properties of concrete slabs

	h mm	d_x mm	d_y mm	f_{cm} MPa	f_{ctm} MPa	E_{cm} GPa	f_y/f_u MPa	Elonga tion, %	Modulus Es, GPa
<i>S1</i>	55	38	35	36.3	3.3	34.4	543/771	22.2	180
<i>S2-FR-IB</i>	55	38	35	36.3	3.3	34.4	543/771	22.2	180
<i>S3-FR</i>	58	40	37	31.3	3.0	33.2	689/806	14.8	203.4
<i>P215-M1099</i>	57	33	30	31.3	2.4	31.0	689/806	14.8	203.4
<i>P368-M1099</i>	58	32	29	32.9	2.6	31.4	689/806	14.8	203.4
<i>P486-M1099</i>	55	33	30	28.9	2.3	30.3	689/806	14.8	203.4
<i>P215-M1356</i>	58	34	31	32.9	2.6	31.4	689/806	14.8	203.4
<i>P215-M2110</i>	59	42	39	28.9	2.3	30.3	689/806	14.8	203.4

1.3 Test setup

The overall test setup is shown in **Fig. 5**. Due to the large dimensions of the furnace (3m long x 3m wide x 0.75m high), it could not simulate the ISO 834 standard fire curve. Its heating rate is about 20⁰C/min, which is within the practical range of heating rate for steel sections as stipulated in BS 5950-8 [3]. As discussed in **Section 4.2**, the simple design method can be applied for both compartment and standard (ISO 834) fire curves.

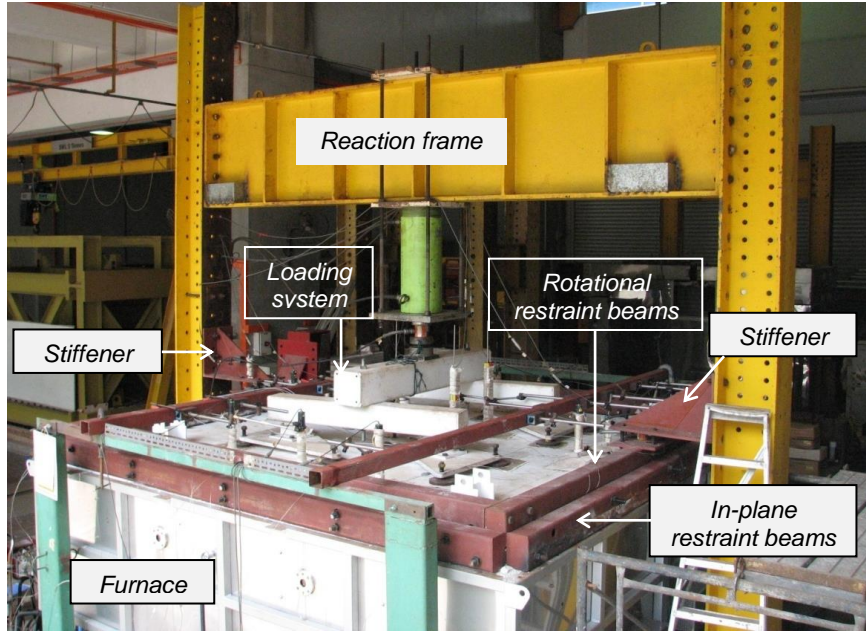


Fig. 5 Typical test setup

1.4 Typical failure mode

Fig. 6 shows a typical crack pattern and final failure mode of a specimen. The failure mode observed in Series I and II was fracture of reinforcement in the slab close to the protected edge beams. As temperature increased, the cracks above the main and secondary edge beams opened widely and penetrated through the slab thickness, leading to reinforcement fracture. No global collapse occurred. No premature failure at the shear studs and at the connections was observed.

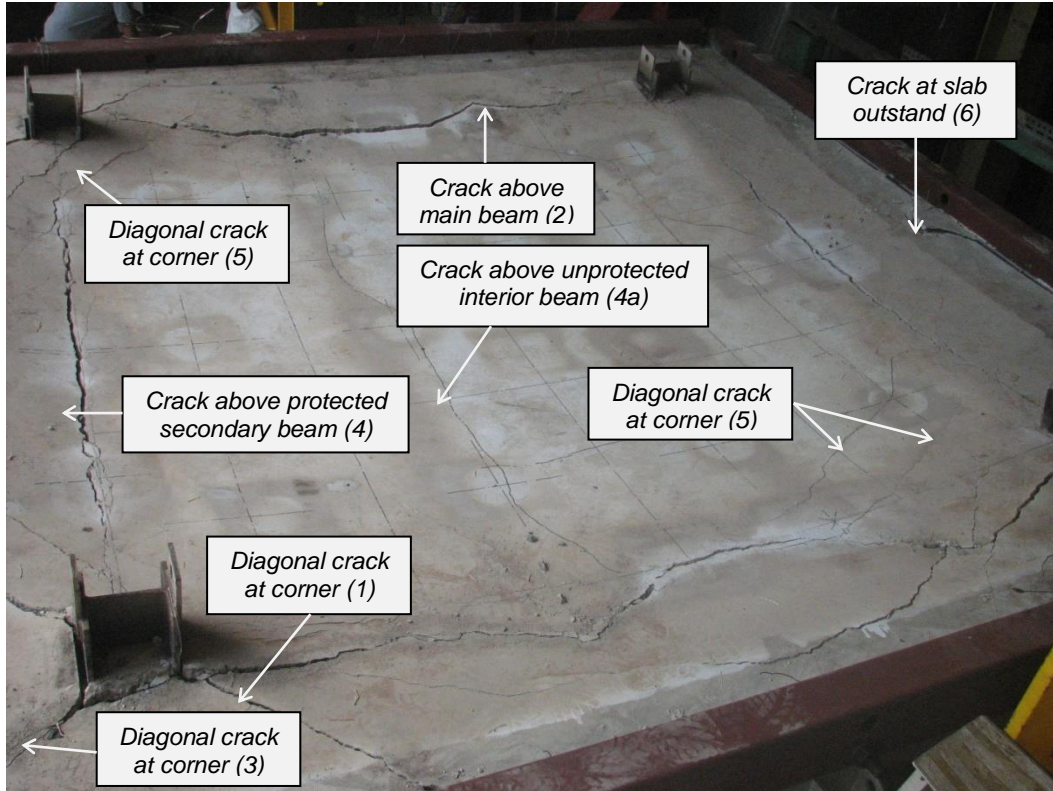


Fig. 6 Typical failure mode

1.5 Validation of the deflection limit

Two deflection limits, *i.e.* the P288 and P390 deflection limits, have been compared to the maximum deflection recorded in the tests (**Table 11**). It should be noted that both deflection limits are calculated by using Eq. (1). The difference lies in the term $(T_2 - T_1)$. SCI P288 assumes that $(T_2 - T_1)$ is equal to 770°C for fire exposure below 90 minutes and 900°C thereafter, while SCI P390 determines T_2 and T_1 based on the temperatures at the bottom and the top surface of the slab, respectively. In the comparison, T_2 and T_1 are determined based on the test results.

$$w = \frac{\alpha(T_2 - T_1)l^2}{19.2h} + \sqrt{\left(\frac{0.5f_y}{E_s}\right)_{\text{Reinf}_{20^\circ\text{C}}}} \frac{3L^2}{8} < w_{\text{max}} = \frac{\alpha(T_2 - T_1)l^2}{19.2h} + \frac{l}{30} \quad (1)$$

In all the cases considered, the deflection limits proposed by P288 [4] and P390 [5] are smaller than the maximum deflections recorded in the tests. In Series I and II, failure of the slab did occur (**Fig. 6**), and all the tests were terminated when fracture of mesh

reinforcement had been identified. Therefore, it can be concluded that the deflection limits proposed by Bailey *et al.* [4] and SCI P390 [5] are conservative.

Table 11 Comparison of deflection limits from SCI P288 and SCI P390

<i>Test</i>	<i>Slab depth</i>	<i>Deflection due to thermal curvature</i>	<i>Deflection due to mechanical strain</i>	<i>P288 deflection limit (Eq. (1))</i>	<i>P390 deflection limit</i>	<i>Max. deflection in test*</i>	<i>P288 deflection limit / Test deflection</i>	<i>P390 deflection limit / Test deflection</i>
	<i>mm</i>	<i>mm</i>	<i>mm</i>	<i>mm</i>	<i>mm</i>	<i>mm</i>		
<i>S1</i>	55	44	54	98	80	131	0.75	0.61
<i>S2-FR-IB</i>	55	44	54	98	86	177	0.55	0.49
<i>S3-FR</i>	58	42	57	99	73	115	0.86	0.63
<i>P215-M1099</i>	57	43	57	99	84	124	0.80	0.68
<i>P368-M1099</i>	58	42	57	99	88	118	0.84	0.74
<i>P486-M1099</i>	55	52	57	108	90	139	0.78	0.65
<i>P215-M1356</i>	58	42	57	99	91	121	0.81	0.75
<i>P215-M2110</i>	59	48	57	105	83	143	0.74	0.58

* *Test terminated when fracture of reinforcement had been identified.*

It can be seen that all the specimens failed at a deflection greater than the P288 deflection limit. This indicates that the Bailey-BRE method is conservative with the ratio of prediction-to-test deflection varying from 0.55 to 0.86. The deflection limit from SCI P390 is even more conservative with the ratio of prediction-to-test deflection ranging from 0.49 to 0.75.

1.6 Validation of the Bailey-BRE method against Series I and II

In this section, the predictions of the load-bearing capacity of the slab from the proposed model and from the Bailey-BRE model are compared and discussed.

Since the Bailey-BRE method cannot consider deflection of the edge beams, the enhancement factor predicted by the Bailey-BRE method is calculated based on Eqs. (2) and (3).

$$\text{Absolute slab deflection: } w_m \quad (2)$$

$$\text{Relative slab deflection: } w_r = w_m - \frac{1}{4}(w_{MB1} + w_{MB2} + w_{PSB1} + w_{PSB2}) \quad (3)$$

where w_{MB1} , w_{MB2} are the deflection of two main edge beams corresponding to w_m ; w_{PSB1} , w_{PSB2} are the deflection of two secondary edge beams corresponding to w_m .

1.6.1 Specimens without unprotected interior beams

Based on the above mentioned deflections, following the design procedure in P288, it is possible to calculate the enhancement factor e for the tested specimens. The load-bearing capacity of the slab *without the interior beams* is equal to $e \times p_{y,\theta}$ ($p_{y,\theta}$ is the yield load at failure temperature).

In a total of eight specimens, there were two without interior beams, i.e. S1 and S3-FR (**Fig. 3**). At the loading phase, the two specimens were loaded to a value of 15.8kN/m², corresponding to a load ratio of about 2.0 for S1 and S3-FR, respectively. **Table 12** summarises the comparison results, which indicates that if using the absolute slab deflection (Eq. (2)), the Bailey-BRE method over-predicts the test results by about 4%, whereas the method is conservative if using the relative slab deflection (Eq. (3)).

Table 12 Comparison of the Bailey-BRE prediction against the specimens without interior beams

Test	P_{test} kN/m ²	MB Defl. mm	PSB Defl. mm	Slab Defl. mm	Relative defl. mm	Total capacity (kN/m ²)		Prediction / Test	
						(Eq. 2)	(Eq. 3)	(Eq. 2)	(Eq. 3)
S1	15.6	28	58	131	88	15.8	13.1	1.01	0.84
S3-FR	16.0	33	28	115	85	17.1	14.6	1.07	0.92
						M =	1.04	0.89	

1.6.2 Specimens with two unprotected interior beams

The 4th assumption of the Bailey-BRE method is that the load-carrying capacity of *the composite unprotected interior beams* and the slab (enhanced due to membrane action) are added together provided that the unprotected interior beams have not failed yet. The

load-carrying capacity of the slab *with the interior beams* can be calculated using Eq. (4).

$$q_{t,\theta} = e \times p_{y,\theta} + p_{b,\theta} \quad (4)$$

where $q_{t,\theta}$ is the total capacity of the slab at temperature θ ; e is the enhancement factor; $p_{y,\theta}$ is the yield load at temperature θ ; $p_{b,\theta}$ is the increase in the slab load capacity due to flexural strength of the unprotected interior beams at temperature θ if these beams have not failed.

The load-carrying capacity of *composite unprotected interior beam* refer to the bending moment resistance of the beam which is calculated using I-steel section plus concrete flange on top of the steel section.

In a total of eight specimens, six specimens which had two unprotected interior beams (**Fig. 4**) were tested. At the loading phase, these specimens were loaded to a value of 15.8kN/m². This load was kept constant and then temperature was increased up to failure. At failure, the load of 15.8kN/m² would be supported by tensile membrane action mobilised in the slab together with any residual flexural resistance of unprotected interior beams. Therefore, the steps to validate the Bailey-BRE method against the specimens with interior beams are as follows:

- Check if the interior beams have failed yet using the bending moment capacity method in BS EN 1994-1-2 [6].
- If the beams had failed, the load of 15.8kN/m² was totally resisted by the slab. The Bailey-BRE enhancement factor is calculated and compared with the enhancement factor determined from the test.
- If the interior beams had not failed yet, the load supported by the interior beams would be subtracted from the test load of 15.8 kN/m². The remainder load was used to calculate the actual enhancement factor and then compared to the predictions by the Bailey-BRE method.

When calculating part of the load supported by the unprotected interior beams, two cases are considered, viz. Case 1 – treating the interior beams as composite beams with part of concrete slab lying above the steel beam, and Case 2 – bare steel beam.

Case 1: Unprotected interior beam is treated as a composite beam

Table 13 shows the verification results of unprotected interior beam (USB). The bending resistance of USB ($M_{Rd,\theta}$) is calculated using its composite section (bare steel beam with part of concrete slab lying above the steel beam) and compared with the design bending moment of the beam under fire conditions to determine whether the beam is failed or not. It should be noted that these specimens had two interior beams; both are taken into account in the calculation.

Table 13 Verification of bending resistance of unprotected interior beam based on composite section

<i>Test</i>	<i>Temp. of USB</i>	<i>Temperature of slab (°C)</i>			$M_{Ed,\theta}$ kNm	$M_{Rd,\theta}$ kN/m ²	<i>Check USB*</i>	$p_{b,\theta}$ kN/m ²
		θ_t	θ_m	θ_b				
<i>S2-FR-IB</i>	892	95	512	664	7.2	5.8	<i>failed</i>	0.0
<i>P215-M1099</i>	761	108	348	602	7.4	14.7	<i>not failed</i>	20.7
<i>P368-M1099</i>	814	118	316	688	7.2	10.0	<i>not failed</i>	14.1
<i>P486-M1099</i>	819	164	478	748	7.5	9.4	<i>not failed</i>	13.3
<i>P215-M1356</i>	842	101	351	734	7.3	12.2	<i>not failed</i>	12.2
<i>P215-M2110</i>	777	228	508	715	7.4	13.2	<i>not failed</i>	18.6

where $M_{Ed,\theta}$ is design bending moment of the interior beam in fire; $M_{Rd,\theta}$ is bending resistance of the composite interior beam in fire; $p_{b,\theta}$ is the increase in the slab load capacity due to flexural strength of the unprotected beams.

Using the results shown in **Table 13**, the total capacity of the floor system can be predicted. The Bailey-BRE prediction is calculated with two different deflections of the slab: absolute deflection (Eq. (2)), and relative deflection (Eq. (3)). **Table 14** indicates that in six specimens, only the prediction for S2-FR-IB is conservative. Therefore, it can

be concluded if the unprotected interior beams are calculated as a composite beam, the total capacity of the floor system predicted by the Bailey-BRE method is not conservative.

Table 14 Comparison of the Bailey-BRE prediction against the specimens with interior beams – Case 1: Unprotected interior beam is calculated as a composite beam

<i>Test</i>	<i>P_{test}</i> kN/m ²	<i>MB defl.</i> mm	<i>PSB defl.</i> mm	<i>Slab defl.</i> mm	<i>Relative defl.</i> mm	<i>Total capacity (kN/m²)</i>		<i>Prediction / Test</i>	
						<i>Bailey (Eq. 2)</i>	<i>Bailey (Eq. 3)</i>	<i>Bailey (Eq. 2)</i>	<i>Bailey (Eq. 3)</i>
<i>S2-FR-IB</i>	15.1	56	84	177	107	14.0	10.4	0.92	0.69
<i>P215-M1099</i>	15.6	38	57	124	76	38.7	34.9	2.48	2.23
<i>P368-M1099</i>	15.3	51	83	118	51	31.4	26.0	2.05	1.70
<i>P486-M1099</i>	15.5	55	94	139	64	31.9	26.1	2.06	1.68
<i>P215-M1356</i>	15.4	59	88	121	48	30.3	24.5	1.97	1.59
<i>P215-M2110</i>	15.6	39	79	143	84	35.2	31.7	2.26	2.03

$$M = \quad \mathbf{1.96} \quad \mathbf{1.66}$$

Case 2: Unprotected interior beam is calculated as a steel beam

Table 13 shows the verification results of unprotected interior beam (USB), in which the bending resistance of USB ($M_{Ed,\theta}$) is calculated using its steel section.

Table 15 Check the capacity of unprotected interior beam using its steel section

<i>Test</i>	<i>Temp of USB</i>	<i>Temperature of slab (°C)</i>			<i>M_{Ed,θ}</i> kNm	<i>M_{Rd,θ}</i> kNm	<i>Check USB</i>	<i>p_{b,θ}</i> kN/m ²
		<i>θ_t</i>	<i>θ_m</i>	<i>θ_b</i>				
<i>S2-FR-IB</i>	892	95	512	664	7.2	1.9	<i>failed</i>	0
<i>P215-M1099</i>	761	108	348	602	7.4	4.9	<i>failed</i>	0
<i>P368-M1099</i>	814	118	316	688	7.2	3.2	<i>failed</i>	0
<i>P486-M1099</i>	819	164	478	748	7.5	3.1	<i>failed</i>	0
<i>P215-M1356</i>	842	101	351	734	7.3	2.8	<i>failed</i>	0
<i>P215-M2110</i>	777	228	508	715	7.4	4.3	<i>failed</i>	0

where $M_{Ed,\theta}$ is design bending moment of the interior beam in fire; $M_{Rd,\theta}$ is bending moment resistance of the steel interior beam in fire; $p_{b,\theta}$ is the increase in the slab load capacity due to flexural strength of the unprotected beams.

The comparison between the Bailey-BRE predictions against test results for Case 2 is shown in **Table 16**. It can be seen that even when the interior beams are treated as steel beams, if using the absolute deflection of the slab, i.e. the deflection of the edge beams is not taken into account, the Bailey-BRE method is not conservative. The prediction is greater than the test about 11%. If using the relative deflection (Eq. (3)), the Bailey-BRE method is conservative.

Table 16 Comparison of the Bailey-BRE prediction against the specimens with interior beams – Case 2: Unprotected interior beam is calculated as a steel beam

<i>Test</i>	<i>p_{test}</i> kN/m ²	<i>MB</i> <i>defl.</i> mm	<i>PSB</i> <i>defl.</i> mm	<i>Slab</i> <i>defl.</i> mm	<i>Relative</i> <i>defl.</i> mm	<i>Total capacity</i> (kN/m ²)		<i>Prediction / Test</i>	
						<i>Bailey</i> (Eq. 2)	<i>Bailey</i> (Eq. 3)	<i>Bailey</i> (Eq. 2)	<i>Bailey</i> (Eq. 3)
<i>S2-FR-IB</i>	15.1	56	84	177	107	14.0	10.4	0.92	0.69
<i>P215-M1099</i>	15.6	38	57	124	76	18.0	14.2	1.15	0.91
<i>P368-M1099</i>	15.3	51	83	118	51	17.3	11.9	1.13	0.78
<i>P486-M1099</i>	15.5	55	94	139	64	18.7	12.9	1.20	0.83
<i>P215-M1356</i>	15.4	59	88	121	48	18.1	12.2	1.17	0.79
<i>P215-M2110</i>	15.6	39	79	143	84	16.6	13.1	1.07	0.84

$$M = \mathbf{1.11} \quad \mathbf{0.81}$$

In summary, the following points can be drawn:

- (i) For the specimens without interior beams, if using the absolute deflection of the slab, the Bailey-BRE method gives a slightly higher prediction compared to the test results (about 4%), whereas the method is conservative if using the relative slab deflection.
- (ii) For the specimens with two interior beams, if the unprotected interior beams are treated as a composite beam, the Bailey-BRE approach gives an un-

conservative prediction. Therefore, it can be concluded that the unprotected interior beams should not be treated as composite beams when taking into account the contribution of the interior beams into the load-bearing capacity of the beam-slab system.

- (iii) For the specimens with two interior beams, if the interior beams are treated as steel beams and using the absolute slab deflection determined from the test, the results predicted by the Bailey-BRE method are greater than the test results about 11% in average. If using the relative deflection, the Bailey-BRE method is conservative.

2. Calibration of the Bailey-BRE method against test series III, IV and V

2.1 Test Series III, IV & V

According to previous parametric study, the slab aspect ratio and boundary continuity were identified as the most important parameters, which may influence the development of tensile membrane action in composite slabs. Therefore, Series III, IV and V were purposely designed to investigate these two parameters.

2.1.1 Specimen details

Series III focused on isolated composite slab-beam systems, and no boundary continuity was considered. In Series IV & V, various boundary conditions were investigated, such as interior (four continuous edges), edge (three continuous edges) and corner (only two continuous edges) panels as indicated in **Fig. 7**. For Series IV and V, different aspect ratios 1.0 and 1.5 were considered, respectively, as shown in **Table 17**.

Table 17 Specimen specifications

Series	Specimen	LxWxT	L/W (aspect ratio)	Supporting steel beams
III	ISOCS1	2250x2250x60mm	1.0	Joist 102x102x23 kg/m
	ISOCS2	2250x2250x60mm	1.0	Joist 102x102x23 kg/m
	ISOCS3	2250x1500x60mm	1.5	Joist 102x102x23 kg/m
IV	ICS1	2250x2250x60mm	1.0	Joist 102x102x23 kg/m

	ECS1	2250x2250x60mm	1.0	Joist 102x102x23 kg/m
	CCS1	2250x2250x60mm	1.0	Joist 102x102x23 kg/m
V	ICS2	2250x1500x60mm	1.5	Joist 102x102x23 kg/m
	ECS2	2250x1500x60mm	1.5	Joist 102x102x23 kg/m
	CCS2	2250x1500x60mm	1.5	Joist 102x102x23 kg/m

where L=length W=width T=thickness in mm;

ISOCS= Isolated composite slab ICS=Interior composite slab

ECS=Edge composite slab CCS=Corner composite slab

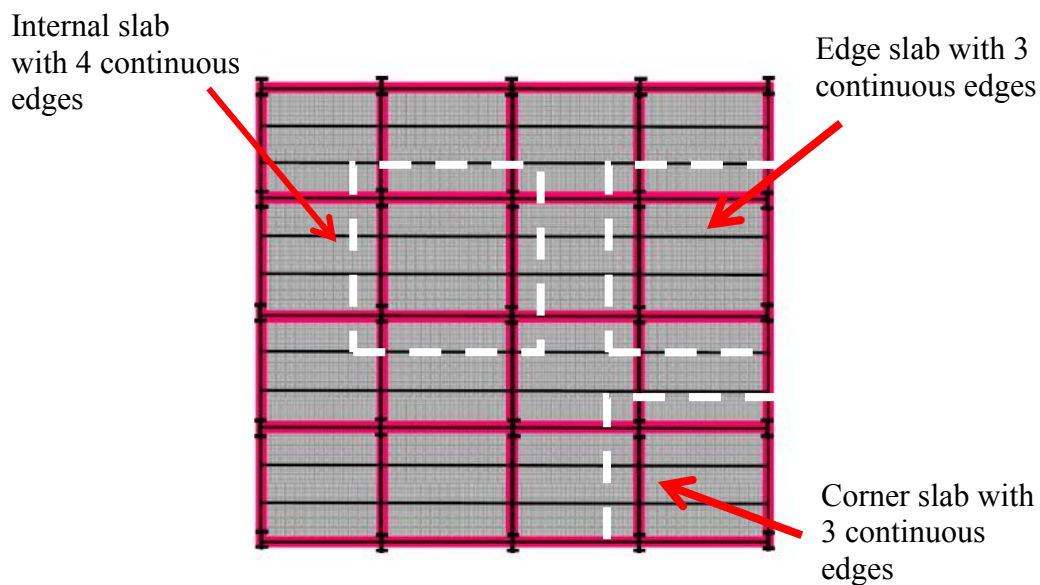


Fig. 7 Typical building layout with different boundary conditions

In order to simulate the boundary continuity, embedded M25 bolts were tied to surrounding restrained frames to ensure the boundary lines remained straight without any movement for both compressive membrane action and tensile membrane action. Moreover, the contacting area between these M25 bolts and concrete was larger than that between the $\Phi 6$ mm mesh and concrete, which was to ensure the edge continuity. Based on the test results, this special tailored boundary design was found to be effective to restrain the edges of composite slabs [1]. Restrained edges were still remained straight after the tests for Series IV and V. However, unrestrained edges were pulled inward at the large deformations. Details of the Series III, IV and V specimens are shown in **Figs. 11-13**.

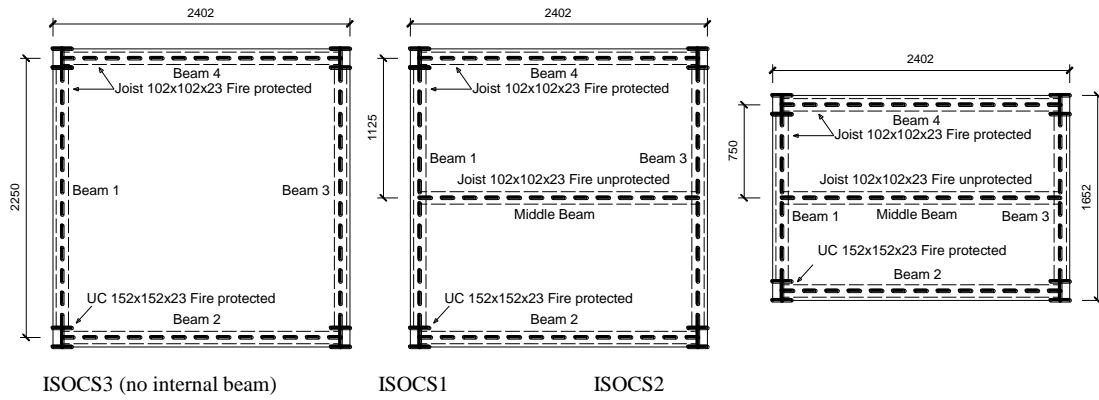


Fig. 8 Specimen details for Series III

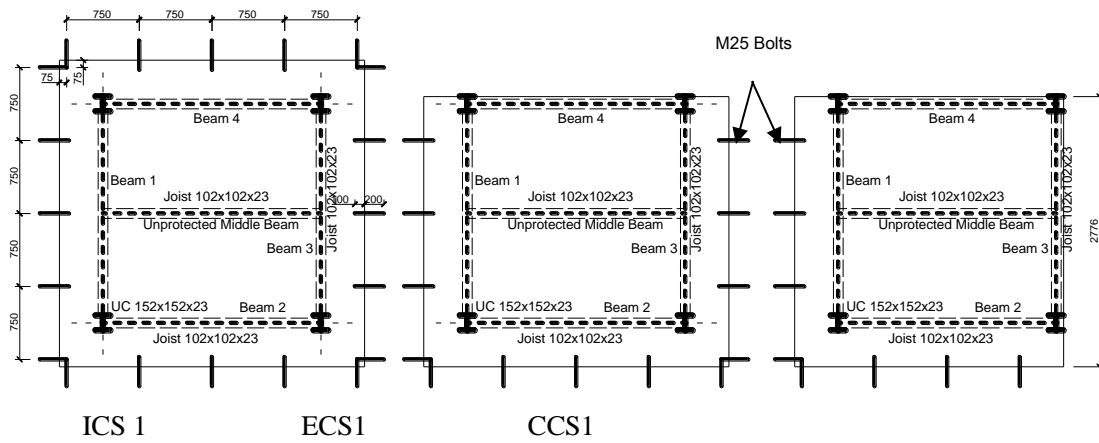


Fig. 9 Specimen details of Series IV

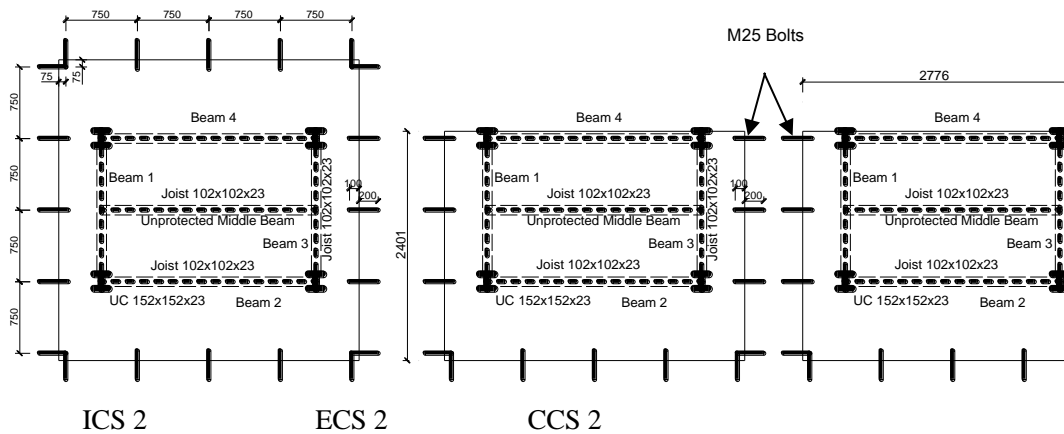


Fig. 10 Specimen details of Series V

2.1.2 Applied load

There are three types of test specimen which are the composite slabs with aspect ratio one without interior beam, aspect ratio of one with interior beam and aspect ratio of 1.5 with interior beam as shown in **Fig. 11**. The yield line loadings for each type of the composite slabs are calculated based on Johansen's yield line theory and summarised in **Table 18**.

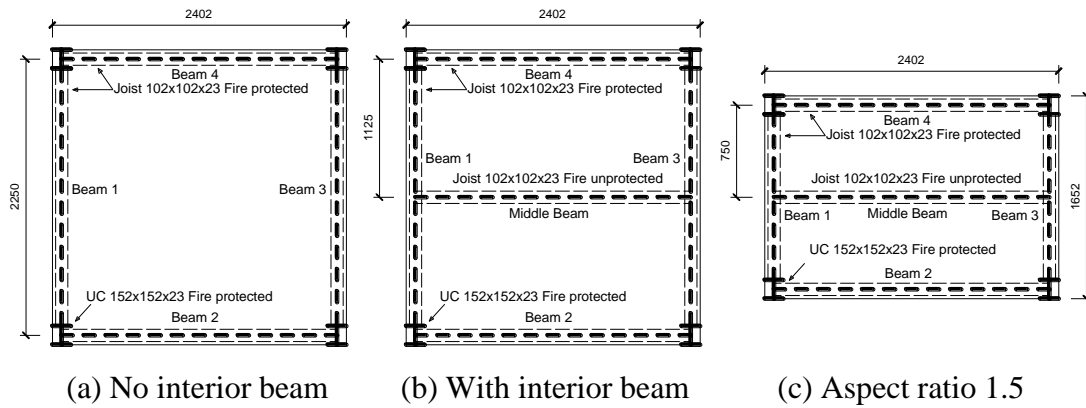


Fig. 11 Three types of test specimens

Table 18 Summary of the yield-line load for three types of specimens

	Yield Line Load
Aspect ratio = 1 without interior beam	11 kN/m ²
Aspect ratio = 1 with interior beam	26 kN/m ²
Aspect ratio = 1.5 with interior beam	48 kN/m ²

The normal practice for composite slabs design load is around 0.4 to 0.6 of the yield line load. Therefore, the applied load was fixed at **20 kN/m²** on the 2400x2400 mm composite slab surface (aspect ratio equal to 1) and **30 kN/m²** on the 2400x1600 mm composite slab surface (aspect ratio equal to 1.5).

In addition, strain gages were attached on the four supporting circular hollow section (CHS) columns, and reaction forces were therefore monitored and calculated to ensure the load system was in equilibrium. **Fig. 12** showed that the reactions in these four

columns were quite uniform and the total reaction forces were consistent with the applying load. After 30 minute, the total reaction forces started to deviate from the apply loading because of the column rotations. The rotation angle measured at the failure point was about 25 degree, which revealed that the total reaction forces should equal to applying load 100kN divided by $\cos(25^\circ)$, which was about 110kN. Therefore, the loading system showed very good agreement with measured reactions.

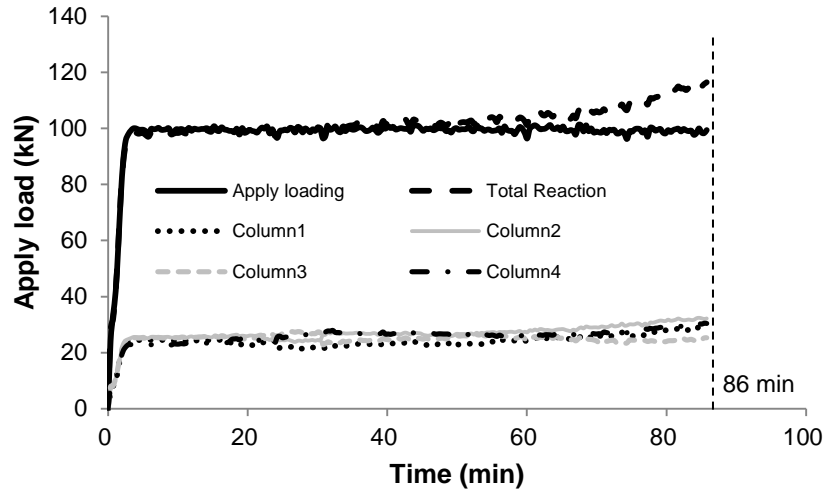


Fig. 12 Applied versus reaction forces

2.1.3 Failure mode

The failure is governed by the (R) load bearing capacity as shown in **Fig. 13**. In this ISOCS3 test, hydraulic pump was used to keep constant 100 kN on the slab surface. However, the apply load started to drop from 86 min. Although the author tried his best to pump back to 100 kN, the measured apply load from load cell still could not restore 100 kN. Then, this 86 min was defined as the failure time for specimen ISOCS3. Therefore, the failure times were all defined in this way for the remaining specimens. In addition, the cross sectional temperature at bottom of the slab, mesh layer and top surface were recorded at the failure time.

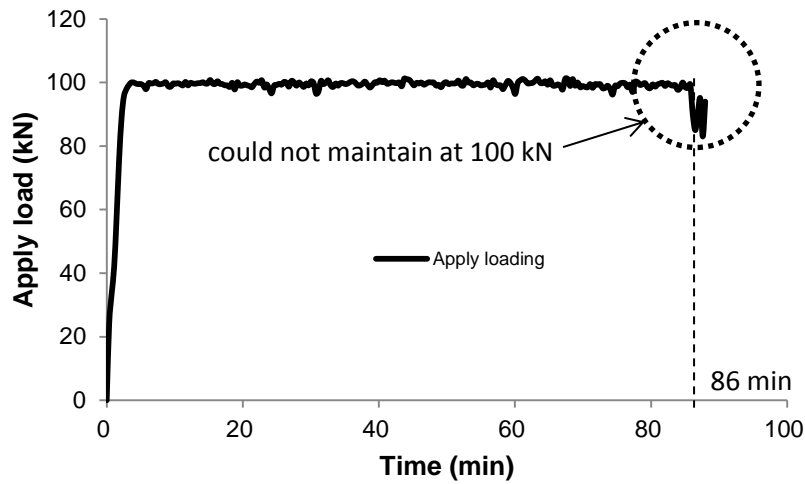


Fig. 13 The applying load versus time for ISOCS3

2.2 Validation of the Bailey-BRE method against Series III, IV and V

The test results of Series III, IV and V are compared with the Bailey-BRE predictions using three following deflections:

- Deflection limit calculated by Eq. (1);
- Absolute deflection measured from the tests (Eq. (2));
- Relative deflection calculated by Eq. (3)

For Series III, IV and V, the calculation principles are the same as Series I and II. The bending resistance of interior beams is calculated to check if these beams have failed yet using the bending moment capacity method in BS EN 1994-1-2. If the beams had failed, the test load was totally resisted by the slab. The enhancement factor calculated by the Bailey-BRE method is calculated and compared with that determined from the fire test.

As shown in Series I and II, the unprotected interior beams should be treated as steel beams. Therefore, for Series III, IV and V, the unprotected interior beams are calculated as *steel beams*.

2.2.1 Comparison of the Bailey-BRE prediction against Series III, IV and V using the deflection limit

Table 19 shows the verification results of unprotected interior beam (USB) in which the bending resistance of USB ($M_{Rd,\theta}$) is calculated using its steel section. Temperatures of the interior beam and the slab are taken at the time when the deflection limit (calculated by Eq. (1)) was reached.

Table 19 Verification of the bending resistance of unprotected interior beam using its steel section (at the deflection limit)

Series	Specimen	Time	USB	Mesh	Slab top	Slab bottom	$M_{Ed,\theta}$	$M_{Rd,\theta}$	Check USB	$p_{b,\theta}$
		min	$^{\circ}C$	$^{\circ}C$	$^{\circ}C$	$^{\circ}C$	kN/m ²	kN/m ²		kN/m ²
<i>III</i> <i>Isolated</i>	ISOCS3	55	N.A.	330	84	672	N.A.	N.A.	N.A.	N.A.
	ISOCS1	60	807	295	97.6	680	6.25	2.96	<i>failed</i>	0
	ISOCS2	59	812	200	98.5	621	6.25	3.4	<i>failed</i>	0
<i>IV</i> <i>Aspect ratio 1</i>	ICS1	75	802	250	98.7	654	6.25	3.0	<i>failed</i>	0
	ECS1	62	796	204	75.8	663	6.25	3.0	<i>failed</i>	0
	CCS1	57	798	191	91.2	689	6.25	3.16	<i>failed</i>	0
<i>V</i> <i>Aspect ratio 1.5</i>	ICS2	58	790	156	89.3	621	6.25	3.99	<i>failed</i>	0
	ECS2	63	800	147.6	99	710	6.25	3.6	<i>failed</i>	0
	CCS2	58	810	138.7	75.5	670.2	6.25	3.44	<i>failed</i>	0

Because the bending resistance $M_{Rd,\theta}$ of USB in all specimens was smaller than the design bending moment $M_{Ed,\theta}$, the unprotected interior beams were failed. Therefore, the increase in the slab load-bearing capacity due to flexural strength of USB, $p_{b,\theta}$, is equal to zero. In other words, the slab was subjected to the whole test load.

Temperatures at the reinforcement mesh, the slab top and bottom surfaces were used to calculate the slab yield line capacity at the deflection limit ($p_{y,\theta}$). The enhancement factor e was then calculated based on the deflection limit.

Table 20 Calibration of the Bailey-BRE method for Series III, IV and V using the deflection limit

Series	Specimen	P_{test}	$P_{y,\theta}$	Slab deflection	Enhancement factor e	Total capacity	Prediction / Test	
		kN/m^2	kN/m^2	w_m		$eP_{y,\theta}$		
				mm		kN/m^2		
<i>III</i> <i>Isolated</i>	ISOCS3	20	10.68	67	1.56	16.67	0.83	
	ISOCS1	20	10.69	69	1.58	16.9	0.85	
	ISOCS2	30	19.24	52.7	1.35	26	0.87	
<i>IV</i> <i>Aspect ratio 1</i>	ICS1	20	10.64	68	1.57	16.72	0.84	
	ECS1	20	10.67	68.3	1.57	16.74	0.84	
	CCS1	20	10.6	69.8	1.58	16.8	0.84	
<i>IV</i> <i>Aspect ratio 1.5</i>	ICS2	30	19.25	52	1.34	25.9	0.86	
	ECS2	30	19.21	54.5	1.36	26.3	0.88	
	CCS2	30	19.25	54.1	1.36	26.4	0.88	
$M =$							0.85	

It can be seen in **Table 20** that the prediction/test load ratio for all specimens is smaller than 1.0. Therefore, it can be concluded that the Bailey-BRE prediction is conservative if using the deflection limit (Eq. (1)).

2.2.2 Comparison of the Bailey-BRE prediction against Series III, IV and V using the absolute deflection

As discussed above, firstly it is necessary to check the bending resistance of USB at the failure point. **Table 21** shows the verification results of USB in which temperatures of the interior beam and the slab are taken at the time when failure occurred.

Table 21 Verification of the bending resistance of unprotected interior beam using its steel section (at the failure point)

Series	Specimen	Failure time	Interior beam	Mesh	Slab top	Slab bottom	$M_{Ed,\theta}$	$M_{Rd,\theta}$	Check USB	$P_{b,\theta}$
		min	$^{\circ}C$		$^{\circ}C$	$^{\circ}C$	$^{\circ}C$	kN/m^2		kN/m^2
<i>III</i>	ISOCS3	86	N.A.	330	84	672	N.A.	N.A.	N.A.	N.A.
	ISOCS1	98	845	465	124	775	6.25	2.47	failed	0

<i>Isolated</i>	ISOCS2	84	925	300	100	870	6.25	1.8	<i>failed</i>	0
<i>Series IV</i>	ICS1	120	945	500	120	900	6.25	1.44	<i>failed</i>	0
	ECS1	84	920	400	110	908	6.25	1.58	<i>failed</i>	0
<i>Aspect ratio 1</i>	CCS1	80	880	320	105	880	6.25	1.97	<i>failed</i>	0
	ICS2	111	950	360	120	920	6.25	1.64	<i>failed</i>	0
<i>Series V</i>	ECS2	124	940	320	118	921	6.25	1.7	<i>failed</i>	0
	CCS2	128	942	300	110	920	6.25	1.7	<i>failed</i>	0

Similarly, the Bailey-BRE predictions are calculated and compared with the test results using the absolute deflection measured from the tests as shown in **Table 22**.

Table 22 Calibration of the Bailey-BRE method for Series III, IV and V at the failure point using the absolute deflection

Series	Specimen	P_{test} kN/m^2	$P_{y,\theta}$ kN/m^2	Slab deflection w_m mm	Enhancement factor e	Total capacity $eP_{y,\theta}$ kN/m^2	Prediction / Test
<i>III</i> <i>Isolated</i>	ISOCS3	20	9.94	178	2.66	26.47	1.32
	ISOCS1	20	7.89	208	2.96	23.34	1.17
	ISOCS2	30	19.25	189	2.47	47.62	1.59
<i>IV</i> <i>Aspect ratio 1</i>	ICS1	20	7.06	184	2.72	19.2	0.96
	ECS1	20	8.72	190	2.77	24.13	1.21
	CCS1	20	9.5	179	2.66	25.27	1.26
<i>IV</i> <i>Aspect ratio 1.5</i>	ICS2	30	17.48	153	2.18	38.05	1.27
	ECS2	30	17.97	158	2.21	39.87	1.33
	CCS2	30	19.21	160	2.24	42.94	1.43

$$M = 1.28$$

It can be seen that the predicted total capacity is significantly greater than the test load for all specimens except ICS1. This is because the Bailey-BRE method assumes that all the four edges are rigid without any deformation. However, in the tests the deformations of four edge beams were revealed. Therefore, the relative slab deflection should be used to calculate the enhancement factor e as discussed in **Section 4.4.2.3**. On the other hand, it can be concluded that the Bailey-BRE method is not conservative if using the absolute deflection measured at the failure point.

2.2.3 Comparison of the Bailey-BRE prediction against Series III, IV and V using the relative deflection

Using the relative slab deflection calculated by Eq. (3), the total capacity of the floor system can be determined and shown in **Table 23**.

Table 23 Calibration of the Bailey-BRE method for Series III, IV and V at the failure point using the relative deflection

Series	Specimen	P_{test} kN/m^2	P_{yield} $line, \theta$ kN/m^2	Slab deflection w_m mm	Average beam deflection mm	Relative slab deflection mm	Enhance ment factor e	Total capacity $eP_{y,\theta}$ kN/m^2	Prediction / Test
III	ISOCS3	20	9.94	178	83	95	1.84	18.28	0.91
	ISOCS1	20	7.89	208	80	128	2.16	17.09	0.85
	ISOCS2	30	19.25	189	130	59	1.4	27.03	0.90
IV	ICS1	20	7.06	184	24	140	2.29	16.12	0.81
	ECS1	20	8.72	190	58	122	2.10	18.29	0.91
	CCS1	20	9.5	179	81	98	1.86	17.68	0.88
IV	ICS2	30	17.48	153	68	85	1.61	28.03	0.93
	ECS2	30	17.97	158	83	75	1.54	27.6	0.92
	CCS2	30	19.21	160	91	69	1.47	28.2	0.94

$$M = 0.89$$

It has been observed that the prediction/test ratios for all specimens are smaller than 1.0. Therefore, the Bailey-BRE method is conservative if using the relative deflection.

3. Conclusions

(1) The Bailey-BRE method

In this section, the calibration of the Bailey-BRE method against the test results from five series is conducted. The method has been verified using three deflection limits:

- Deflection limit proposed in SCI P288 [7] and SCI P390 [5] (Eq. (1))
- Absolute slab deflection measured from the tests (Eq. (2))
- Relative slab deflection measured from the tests (Eq. (3))

The results are summarised in **Table 24**.

Table 24 Summary of calibration results for the Bailey-BRE method against five test series

Test series	USB is treated as a composite beam			USB is treated as a steel beam		
	Deflection limit proposed in SCI P288& P390	Absolute deflection	Relative deflection	Deflection limit proposed in SCI P288& P390	Absolute deflection	Relative deflection
I	U	U	U	C	U	C
II	U	U	U	C	U	C
III	U	U	U	C	U	C
IV	U	U	U	C	U	C
V	U	U	U	C	U	C

*U: unconservative; C: conservative

As can be seen in **Table 24**, the Bailey-BRE method is shown to be conservative provided that: (1) when calculating the slab enhancement factor, *the deflection limit proposed in SCI P288& P390* or *the relative deflection* of the beam-slab floor systems is used; (2) when calculating the total load-bearing capacity of the beam-slab floor system, the unprotected interior beams are treated as *steel beams*.

(2) *Design procedure*

As discussed above, the comparisons between the predicted results by the Bailey-BRE method and the test results conducted by NTU show that the Bailey-BRE method is conservative provided that the unprotected interior beams are treated as *steel beams*. However, since the residual capacity of unprotected interior beams under fire conditions is very small, it is recommended that the residual capacity of unprotected interior beams under fire conditions is ignored when calculating the load-bearing capacity of composite beam-slab floor systems.

Therefore, the following point in the design procedure should be revised as follows:

*“The load carrying capacity of **the unprotected interior steel beams** under fire conditions is ignored”.*

The revised design procedure is shown in **Fig. 12**.

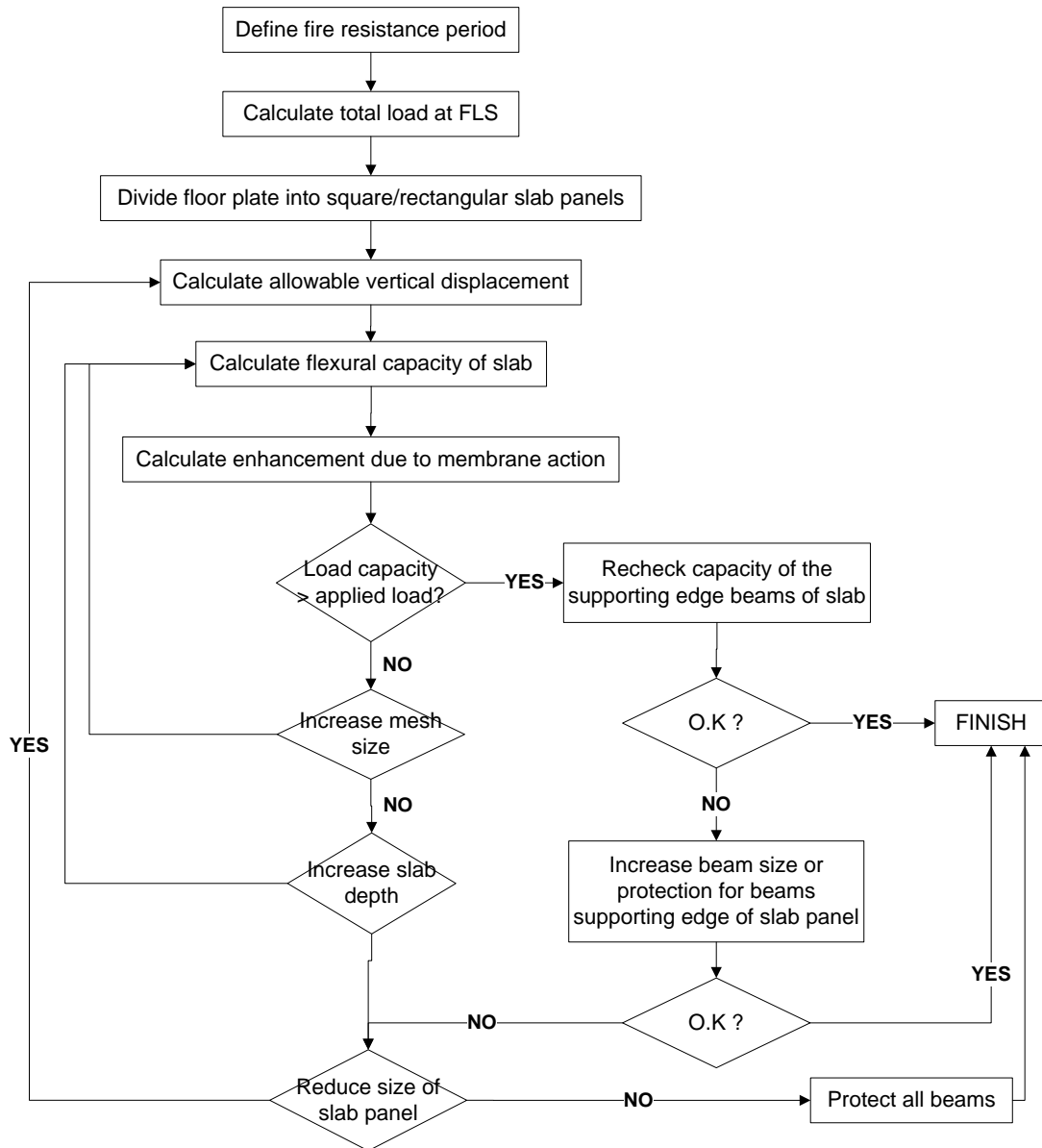


Fig. 14 Revised design procedure of the Bailey-BRE method

References

- [1] Tan KH, Nguyen TT, Liu JX. *Explore Concept of Membrane Action in Slabs to Reduce Fire Protection for Beams*. Project report. Nanyang Technological University, School of Civil and Environmental Engineering. 2013.
- [2] Nguyen T-T. *Behaviour of Composite Slab-Beam Floor Systems under Fire Conditions*. Ph.D. Thesis. Nanyang Technological University; 2013.
- [3] BS 5950-8: *Structural use of steelwork in building. Part 8: Code of practice for fire resistant design*. British Standard Institution (BSI), London, 2003.
- [4] Bailey CG, Moore DB. Structural behaviour of steel frames with composite floorslabs subject to fire: Part 1: Theory. *Structural engineer London*. 2000a;78:19-27.
- [5] Simms WI, Bake S. *TSLAB V3.0 User Guidance and Engineering Update*. The Steel Construction Institute. SCI Publication P390. 2010.
- [6] EN 1994-1-2: *Eurocode 4. Design of composite steel and concrete structures - Part 1-2: General Rules - Structural fire design*. European Committee for Standardization (CEN), Brussels, Belgium, 2005.
- [7] Newman GM, Robinson JT, Bailey CG. *Fire Safe Design: A new Approach to Multi-Story Steel-Framed Buildings*. Technical Report. 2nd: The Steel Construction Institute. SCI Publication P288. 2006.